UNIVERSITÀ DEGLI STUDI DI TRIESTE
GRADUATE SCHOOL OF NANOTECHNOLOGY
XXV CYCLE

DESIGN AND SYNTHESIS OF FUNCTIONALIZED METAL NANOPARTICLES FOR BIO-ANALYSIS WITH SURFACE-ENHANCED RAMAN SCATTERING (SERS)

(SSD: ING-IND/22)

PhD Candidate:
Lucia Marsich

Director of the School:
Prof. Dr. Maurizio Fermeglia

Advisor:
Prof. Dr. Valter Sergo

Tutor:
Dr. Alois Bonifacio

ANNO ACCADEMICO 2011 / 2012

Abstract

The objective of this doctoral research is the development and the implementation of SERS-active substrates with biological samples. The substrates consist in coated silver nanoparticles synthesized by chemical reduction of a silver salt. The biological samples are the anionic chromophore bilirubin and two heme protein, the cationic cytochrome-c and the anionic protein cytochrome b5.

In the first part of this work, positively charged nanoparticles were prepared by coating citrate-reduced silver nanoparticles with the cationic polymer poly-L-lysine and were employed with bilirubin in the experiments listed below:

- detection of nanomolar bilirubin concentrations in aqueous solutions, showing that the SERS intensity increases linearly with concentration in a range from 10 nM to 200 nM, allowing quantitative analysis of bilirubin aqueous solutions.
- indirect quantification of bilirubin cellular up-take, demonstrating the ability to detect the bilirubin also in a buffer solution suitable for cell growth with pH 7.4. Since the bilirubin quantification at this pH is no longer possible, the poly-L-lysine was substituted by two polymers with a quaternary nitrogen atom.
- bilirubin measurement in serum, but TEM images highlights the formation of a albumin layer around the nanoparticles, blocking the interaction between bilirubin and the nanoparticles. Hence the citrate-reduced silver nanoparticles

were coated with an hydrophobic capping and re-dispersed in hexane, to avoid the albumin layer around the nanoparticles.

In the second part of this doctoral thesis, silver nanoparticles were prepared via seed growth method and subsequently coated with chitosan or silica in order to obtain positively or negatively charged nanoparticles respectively. Such substrates enhance the spectrum of the cytochrome-c and cytochrome-b5 on polished silver electrode without directly interact with the protein. Thanks to the presence of chitosan or silica coated nanoparticles, the cytochrome-c and cytochrome-b5 can be detected on a gold substrate.

Sommario

L'obiettivo di questo dottorato è lo sviluppo e l'implementazione di substrati SERS attivi con campioni biologici. Nanoparticelle di argento ricoperte sono state scelte come substrati. I campioni biologici analizzati sono la bilirubina e due proteine eme, il citocromo-c (cationico) e il citocromo-b5 (anionico).

Nella prima parte di questo lavoro le nanoparticelle di argento sono state preparate usando come agente riducente il citrato e successivamente sono state ricoperte con un polimero cationico, la poli-lisina. Le nanoparticelle cariche positivamente così ottenute sono state impiegate con la bilirubina nei seguenti esperimenti:

- rilevazione di concentrazioni nano-molari di bilirubina in soluzioni acquose, dimostrando che per concentrazioni comprese tra 10 e 200 nM, l'intensità degli spettri SERS aumenta linearmente con la concentrazione. È quindi possibile l'analisi quantitativa di bilirubina in soluzioni acquose.
- quantificazione indiretta dell'assorbimento cellulare di bilirubina, documentando la possibilità di rilevare la bilirubina in una soluzione tampone che permetta la crescita cellulare a pH 7.4. Dal momento che la quantificazione della bilirubina in questa soluzione buffer non è più possibile, la poli-lisina è stata sostituita con due polimeri che presentano un azoto quaternario.

- misura della bilirubina nel siero, ma le immagini TEM evidenziano la formazione intorno alle nanoparticelle di uno strato di albumina, che impedisce l'interazione della bilirubina con le nanoparticelle ricoperte di poli-lisina. Per evitare la formazione dello strato di albumina, le nanoparticelle di argento sono state quindi ricoperte con un capping idrofobico e ridisperse in esano.

Nella seconda parte di questa tesi di dottorato, le nanoparticelle di argento sono state preparate a partire da nanoparticelle di qualche nanometro e successivamente ricoperte con chitosano o silice. Lo spettro del citocromo-c e del citocromo-b5 sono stati amplificati grazie alla presenza di queste nanoparticelle senza interagire direttamente con le proteine. Grazie alla presenza delle nanoparticelle ricoperte di chitosano o silice, il citocromo-c e il citocromo-b5 sono stati misurati su un substrato d'oro.

Table of contents

List of abbreviations

4-ATP	4-aminothiophenol
4-MBA	4-mercaptobenzoic acid
AgNPs@Chitosan	chitosan coated silver nanoparticles prepared via seed growth method
AgNPs@SiO_2	silica coated silver nanoparticles prepared via seed growth method
$AgNPs_{405}$	silver nanoparticles with absorption maximum at 405 nm
$AgNPs_{418}$	silver nanoparticles with absorption maximum at 418 nm
AgSEEDs	small silver nanoparticles (for synthesis via seed growth method)
APTS	aminopropyltrimethoxy silane
AUT	11-aminoundecanethiol hydrochloride
Cit-AgNPs	citrate-reduced silver nanoparticles
DLS	dynamic light scattering
DMSO	dimethyl sulfoxide
HSA	human serum albumin

LL-AgNPs	silver nanoparticles synthesized using Leopold-Lendl procedure
MUA	mercaptoundecanoic acid
NPs	silver nanoparticles
ODA	octadecylamine
ODA-Cit-AgNPs	octadecylamine coated citrate-reduced silver nanoparticles
ODA-LL-AgNPs	octadecylamine coated Lee-Meisel silver nanoparticles
P(AAm-DADMAC)	poly(acrylamide-co-diallyldimethylammonium chloride)
P(DADMAC)	poly(diallyldimethylammonium chloride)
PLL	poly-L-lysine
PLL-AgNPs	poly-L-lysine coated citrate-reduced silver nanoparticles
Poly-N^+	polymer with a quaternary nitrogen atom
RR	resonance Raman
SERRS	surface enhanced resonance Raman scattering
SERS	surface enhanced Raman scattering

Chapter 1:

Introduction

In this doctoral thesis the development of nanostructured metal substrates as sensor for biological samples using the Surface Enhanced Resonance Raman Scattering active substrates is presented.

Raman spectroscopy is a non-destructive analytical technique based on the inelastic scattering of a monochromatic light (usually provided by a laser source) by vibrating molecules. This technique is widely used to provide information on chemical structures: i) the identification of a substances is possible from the characteristic spectral patterns (fingerprinting), and ii) the quantification since the spectrum intensity is proportional to the analyte concentration [1]. Samples can be examined in a whole range of physical states as solids, liquids or vapors, ,in bulk, as microscopic particles, or as surface layers. The techniques are very wide ranging and provide solutions to a host of interesting and challenging analytical problems [2]. Unfortunately, the applicability of Raman spectroscopy is limited by its poor sensitivity.

To increase the Raman intensity, analytes can be adsorbed on a nanostructured metal surface with adequate characteristics, yielding a surface-enhanced Raman scattering (SERS) spectrum [3]. If the analyte has an electronic transition in resonance

with the wavelength of the exciting laser, a surface enhanced resonance Raman scattering (SERRS) spectrum is obtained [1], in which both the SERS and the resonance Raman (RR) effects contribute to the enhancement [4,5]. Thus, SERS spectroscopy provides structure-specific vibrational spectra of adsorbates with extremely high sensitivity, the technique also ensures a high selectivity since only adsorbed species can be detected. SERRS provides an additional selectivity, achieved upon tuning the excitation laser in resonance with the analyte of interest, whose Raman spectrum will selectively benefit from the resonance enhancement. Due to these advantageous characteristics SER(R)S has become one of the most promising analytical method for chemical and biochemical detection and analysis [6].

Silver nanoparticles are widely used as efficient SE(R)RS substrates, and a careful control over their surface charge is very important to tune their affinity toward an analyte [7]. One of the most used protocol to prepare Ag nanoparticles for SE(R)RS is the reduction of Ag+ ions with sodium citrate [8,9]. Citrate-reduced colloids are very easily prepared, are stable for months and yield very intense SERS spectra [10]. Due to the adsorbed citrate anions this kind of nanoparticles have a negative surface charge [10]. Another reducing agent to easily prepare silver nanoparticles is hydroxylamine which yields negatively charged colloids [9, 11]. Reduction with $NaBH_4$ yields positively charged Ag nanoparticles, but these colloids are less stable than citrate- reduced ones [9,10,12].

In the following sections the Raman and SE(R)RS spectroscopy will be described with more details and a short review of SE(R)RS active substrate will be reported.

1.1 Short historical recall of the Raman effect

Before addressing the scientific problem, it would seem appropriate to recall its historical background. The inelastic scattering of light by matter was predicted on theoretical grounds by the French scientist Léon Brillouin (1922), and by the Austrian scientist Adolf Smekal (1923), but it was not observed until 1928. The effect took the name of its discoverer, the Indian scientist Chandrasekhra V. Raman. He observed the effect for the first time in 1928 together with K. S. Krishnan using as source light a focused, filtered beam of sunlight and as detector the human eye. In the same year Grigory Landsberg and Leonid Mandelstam reported independently the Raman effect. Raman received the Nobel Prize in 1930 for his work on the scattering of light. The experimental arrangement has not improved significantly until the invention of the laser (Schawlow and Townes, 1958; Maiman, 1960), the ideal source for Raman spectroscopy [2].

1.2 The Raman effect mechanism

When light interacts with matter, the photons maybe absorbed or scattered, or may not interact with the material [2]. According to quantum theory, a molecular motion can have only certain discrete energy states. A change in state is thus accompanied by the gain or loss of one or more quanta of energy. The absorption process involves the gain of a quantum of energy by the molecule, accompanied by the annihilation of a quantum of light or photon. Similarly, spontaneous emission can be described as the creation of one or more photons due to the corresponding loss in molecular energy.

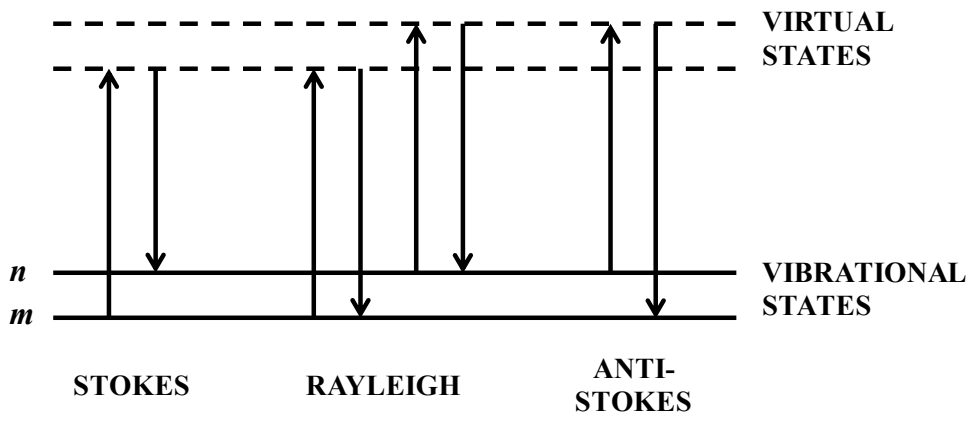

Figure 1: Diagram of the Rayleigh and Raman scattering processes. The lowest energy vibrational state m is shown at the foot with states of increasing energy above it. Both the low energy (upward arrows) and the scattered energy (downward arrows) have much larger energies than the energy of a vibration. [13]

Scattering processes involve at least two quanta acting simultaneously in the light-matter system. Simple elastic scattering (Rayleigh) occurs when a quantum of electromagnetic energy is created at the same time that an identical one is annihilated. In the case of an inelastic process such as the Raman effect, the two photons are not identical and there is a net change in the state of the molecule.

If the created photon is less energetic than the annihilated one, the scattered light is observed at a frequency that is lower than that of the incident light (Stokes Raman scattering). This process leads to absorption of energy by the molecule and its promotion from the ground vibrational state m to a higher energy excited vibrational state n (Figure 1). On the other hand, due to thermal energy, some molecules may be present in an higher excited state n (Figure 1). Scattering from these states to the ground state m involves transfer of energy to the scattered photon. The created photon is more energetic than the annihilated one and the scattered light frequency will be higher (anti-Stokes Raman scattering). The relative intensities of the two processes depend on the population of the various states of the molecule. At room

temperature, the number of molecules expected to be in an excited vibrational state will be small. Thus, compared to Stokes scattering, anti-Stokes scattering will be weak [13]. Since both give the same information, it is customary to measure only the Stokes side of the spectrum.

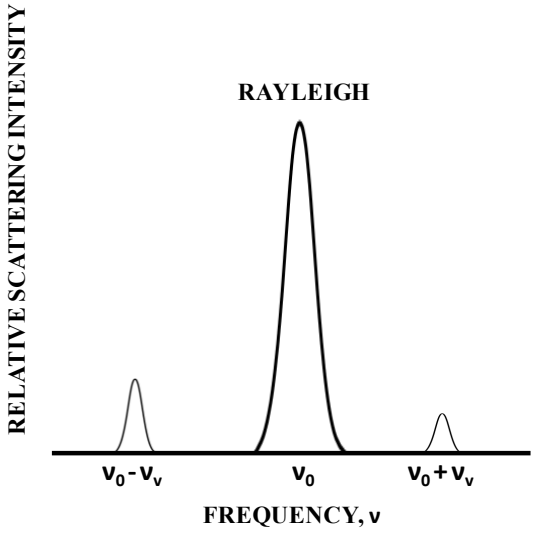

Figure 2: Raman effect: the Rayleigh scattering has the same frequencies of the monochromatic exciting light ν_o; the Raman Stokes and anti-Stokes frequencies depend on the sample molecular vibration frequency ν_v [2].

The scattering processes for diatomic molecule the liquid state, which has only one vibrational frequency (ν_v) is illustrated in Figure 2. The relatively strong Rayleigh line appears at the excitation light frequency ν_0, the Raman bands, 10^{-3} weaker than the Rayleigh and 10^{-6} than the incident light, are the result of inelastic scattering by a molecular vibration of frequency ν_v. The inelastically scattered light constitutes the Raman spectrum of the sample.

The Raman scattering can be explained according to classical theory [14]. The electric field strength (E) of the electromagnetic wave (laser beam) fluctuates in time (t) with an amplitude E_0 and a frequencies ν_0 can be writen as:

1) $$\boldsymbol{E = E_0 \cos 2\pi \nu_0 t}$$

If a diatomic molecule is irradiated by light (laser beam), an electric dipole moment P proportional to E, is induced:

2) $$\boldsymbol{P = \alpha E = \alpha E_0 \cos 2\pi \nu_0 t}$$

The proportionality constant α is called polarizability. If the molecule is vibrating with a frequency ν_m and a q_0 amplitude, the nuclear displacement q is written:

3) $$\boldsymbol{q = q_0 \cos 2\pi \nu_m t}$$

For a small amplitude of vibration, a is a linear function of q:

4) $$\boldsymbol{\alpha = \alpha_0 + \left(\frac{\partial x}{\partial q}\right)_0 q_0 + \cdots}$$

where α_0 is the polarizability at the equilibrium position, and $\left(\frac{\partial x}{\partial q}\right)_0$ is the rate of change of α with respect to the change in q, evaluated at the equilibrium position.

Combining (2) with (3) and (4):

5) $$\boldsymbol{P = \alpha_0 E_O \cos 2\pi \nu_0 t + \left(\frac{\partial x}{\partial q}\right)_0 q_0 E_O \cos 2\pi \nu_0 t \cos 2\pi \nu_m t =}$$

$$\boldsymbol{= \alpha_0 E_O \cos 2\pi \nu_0 t + \frac{1}{2}\left(\frac{\partial x}{\partial q}\right)_0 q_0 E_O \{\cos[2\pi(\nu_0 + \nu_m)]\, t + \cos[2\pi(\nu_0 - \nu_m)]\, t\}}$$

The first term represents an oscillating dipole that radiates light of frequency ν_0 (Rayleigh scattering), while the second term corresponds to the Raman scattering of frequency $(\nu_0 + \nu_m)$ (anti-Stokes) and $(\nu_0 - \nu_m)$ (Stokes).

If the factor $\left(\frac{\partial x}{\partial q}\right)_0$ in the second term of the equation is zero no Raman scattering can occurs. A molecule is Raman active if the polarizability derivate is different from zero. If a vibration does not greatly change the polarizability of the molecule, then the polarizability derivative will be near zero, and the intensity of the Raman band will be weak.

1.3 Resonance Raman

Resonance Raman (RR) scattering occurs when the excitation frequency is close to the analyte electronic transition. In this way the intensities of Raman bands are enhanced by a factor of 10^3 or 10^4. This means that Raman spectroscopy becomes a much more sensitive and selective technique since only the chromophore gives the more efficient scattering [13].

Theoretically, the intensity of a Raman band observed at $(\nu_0-\nu_{mn})$ is given by [14]:

6) $$\boldsymbol{I_{mn} = cost \cdot I_0(\nu_0 - \nu_{mn})^4 \sum_{p\sigma} \left|(\alpha_p)_{mn}\right|^2}$$

The initial and the final state of the electronic ground state are denoted by m and n respectively and *e* represents an electronic excited state. I_0 is the intensity of the incident laser beam with a frequencies ν_0, $(\alpha_{p\sigma})_{mn}$ represents the change in polarizability α caused by the m → e → n transition (Figure 3), p and σ are x, y and z components of the polarizability tensor. The $(\alpha_p)_{mn}$ term can be rewritten as:

7) $$\boldsymbol{(\alpha_p)_{mn} = \frac{1}{h}\sum_e \left(\frac{M_{me}M_{en}}{\nu_{em}-\nu_0+i\Gamma_e} + \frac{M_{me}M_{en}}{\nu_{em}+\nu_0+i\Gamma_e}\right)}$$

where ν_{em} and ν_{en} are the frequencies corresponding to the energy difference between the states *e* and *m* and the states *e* and *n* respectively (Figure 3) and h is

Planck's constant. M_{me}, M_{en} are the electric transition moments; Γ_e is the band width of e state and $i\Gamma_e$ term is called damping constant.

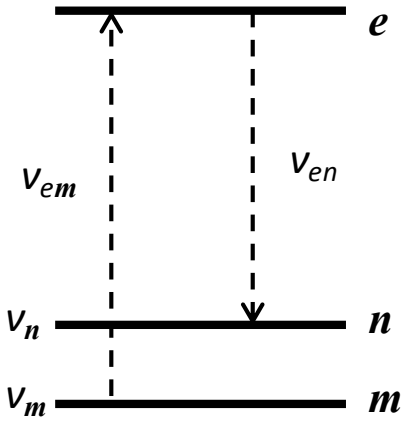

Figure 3: Energy level diagram for resonance Raman transition [14].

In normal Raman scattering, ν_0 is chosen so that $\nu_0 < \nu_{em}$. Under these conditions, the Raman intensity is proportional to $(\nu_0 - \nu_{mn})^4$. As ν_0 approaches ν_{em}, $(\nu_{em} - \nu_0)$ becomes very small. Hence, the first term in the brackets of equation 7), the resonance term, becomes so large that the intensity of the Raman band at $(\nu_0 - \nu_{mn})$ increases enormously. This phenomenon is called resonance Raman (RR) scattering.

1.4 The SERS effect

SERS is a surface-sensitive technique that enhances Raman scattering of molecules adsorbed on nanostructured metal surfaces. The denomination surface-enhanced Raman scattering (SERS) summarizes particularly well these three effect:

– Surface (S): SERS is a surface spectroscopy technique. The molecules must be adsorbed on the metal surface, or at least be very close to it (typically 10 nm

maximum). This is a major point for applications of SERS, ensuring the selectivity if the technique.

– Enhanced (E): the signal enhancement is provided by plasmon resonances in the metal substrate. The term `plasmon resonances' belongs to a family of effects associated with the interaction of electromagnetic radiation with metals. A more detailed description of this phenomena is given in the next section.

– Raman (R): the technique consists in measuring the Raman signals of molecules. A detailed description of the Raman effect itself was given in previous sections.

One of the major characteristics of SERS is its interdisciplinary nature. SERS exists at the boundaries shared among physics, chemistry, colloid science, plasmonics, technology, engineering, and biology [12].

1.5 Short historical recall of the SERS effect

Surface-enhanced Raman scattering (SERS) was discovered in 1974. Fleischman and his colleagues reported the strong Raman scattering from pyridine adsorbed on a silver roughened electrode. The authors attribute the effect to a local increase of the pyridine molecules adsorbed on the roughed surface. Some years later, Jeanmarie and Van Duyne from Northwestern University (USA) and Albrecht and Creighton of the University of Kent (UK) correctly interpreted the intensity enhancement showing that the 10^6 enhancement in the signal intensity is related to an intrinsic surface enhancement effect [3, 13].

1.6 The SERS enhancement mechanism

It is currently widely accepted that two mechanisms contribute to the SERS enhancement: electromagnetic and chemical [15]. The chemical mechanism enhances the Raman-scattering cross section of an analyte directly adsorbed on the metal surface. The enhancement due to the latter mechanism depends on the chemical nature of the analyte and on its adsorption geometry, and it is generally weaker than that due to the electromagnetic mechanism.

From an electromagnetic view point, metals can be considered a plasma composed of polarizable free electron, and positive ion core. The laser light excites the collective oscillations of the surface conduction electrons in a metal (surface plasmons) and the free electron coherently oscillate at the plasmon frequencies (ω_P), as schematically reported in Figure 4. This excitation results in the enhancement of the local electromagnetic field intensity experienced by a molecule adsorbed or in close proximity to the metal surface.

The field induced at the surface of the nanoparticles is given by:

8) $$\boldsymbol{E_{induced}} = \left\{\frac{[\varepsilon_1(\omega)-\varepsilon_2]}{\varepsilon_1(\omega)+2\varepsilon_2}\right\}\boldsymbol{E_{incident}}$$

where $\varepsilon_1(\omega)$ is the complex dielectric function of the metal structure and ε_2 is the relative permittivity of the surrounding medium.

As a consequence of the presence of this secondary electromagnetic field, the intensity of the Raman scattered light is enhanced. It should be stressed that direct adsorption of an analyte on the surface is not needed for this mechanism to operate.

The increased electromagnetic field results in enhanced Raman scattered light (E_R) is given by

9) $$\boldsymbol{E_R = \alpha_R g E_0}$$

where α_R is the fraction of the photons undergoing inelastic scattering under normal conditions and g is the average field enhancement over the particle surface. Furthermore, the Raman-scattered light is also enhanced by a similar process but to a different magnitude (g'). Effectively, the average SERS intensity (ISERS) will be proportional to square of the product of both the gains $I_{SERS} \propto |g \cdot g'|^2$. For low-frequency Raman modes, the gains g and g' can be considered to be almost equal. Hence, the SERS intensity is proportional to the fourth power of the gain in the electromagnetic field caused by the nanostructure.

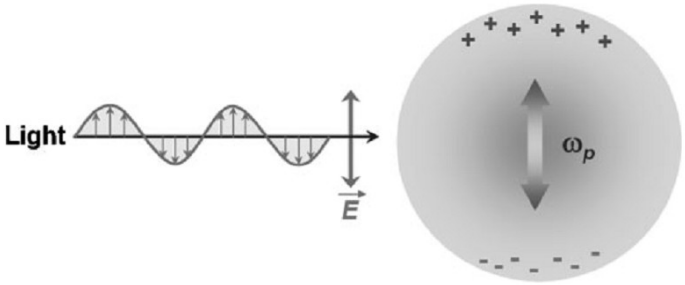

Figure 4: Schematic image of plasmon oscillation for a metal nanoparticle: the interaction of the electromagnetic wave with a metal causes the oscillation of the free electron at the plasmon frequency (ω_P) [15].

1.7 SERRS – Surface Enhanced Resonance Raman Scattering

Besides the chemical and electromagnetic enhancement mechanism, if the analyte has an electronic transition in resonance with the wavelength of the exciting laser, a surface enhanced resonance Raman scattering (SERRS) spectrum is obtained [13]. In this case both the SERS and the resonance Raman (RR) effects contribute to the enhancement, yielding enhancing factors up to 15 order of magnitude [4, 5].

The SERRS signals are often quite similar to those obtained from resonance Raman scattering, with much less evidence of orientation dependence or other surface selection rules. As already said, SERRS spectroscopy provides structure-specific vibrational spectra of adsorbates with extremely high sensitivity; moreover, the technique also ensures an additional selectivity, achieved upon tuning the excitation laser in resonance with the analyte of interest, whose Raman spectrum will selectively benefit from the resonance enhancement.

1.8 SE(R)RS spectra interpretation

The basic components involved in a Raman vibrational spectrum are just the molecule and the incident radiation. In contrast, in SERS, the basic components involved are a molecule, a metal nanostructure and electromagnetic radiation. This difference introduces a much greater degree of complexity to SERS experiments. Several factors must be considered during the interpretation of a SERS spectrum [3]:

- The molecule is interacting with a metal nanostructure. The adsorption on solid surfaces can be divided, according to the strength of bonding between the particle and the substrate, into two categories, physisorption and chemisorption. Physical adsorption (physisorption) refers to weak interactions arising from van der Waals force. When the adsorption energy is large enough and comparable to chemical bond energies (formation of a chemical bond), the term chemisorption is used. In both case, the enhancement will be higher for the molecular groups that directly interact with the metal surface.
- The interaction of incident radiation with adsorbed molecules may lead to photodissociation, photoreactions or simply photodesorption. All of these

processes can leave their own fingerprints in the observed SERS. For instance, the photodissociation of organic molecules on silver nanostructures is characterized by the well-known 'cathedral peaks' of SERS that arise from carbon products on silver.

- The interaction of light with the metallic nanostructure depends on the value of the complex dielectric function at the excitation wavelength, and this will determine the enhancement observed at a given frequency of excitation. Since particle absorption and scattering depend on the shape and size of the metal nanostructure, SERS intensities are also influenced by these factors. In addition, the excitations in nanostructures are strongly influenced by the dielectric constant of the medium.
- The dynamics of the interaction of light with the adsorbate leads to a pattern of Raman intensities determined by selection rules. Surface selection rules cover the symmetry properties of the dipole transitions and the modification of the intensities due to the components of the local electric field vector at the surface.
- SERS is commonly obtained by excitation with visible or near infrared light. The presence of the metal nanostructure may permit new excitations in the molecule–nanostructure complex. Since the excitation is in resonance with the electronic transition of the adsorbed metal complex, the observed inelastic scattering is formally due to a related physical phenomenon: resonance Raman scattering. The observed SERS could indeed be surface-enhanced resonance Raman scattering (SERRS), and the observed relative intensities may not resemble the original Raman spectrum of the parent molecule.

- Finally, small amounts of impurities may burst forth to give sudden signals that further complicate the interpretation of the observed SERS spectra.
- Another important issue in the SERS spectra is the distance dependence of the enhancement effect. The distance dependence of corresponding intensity, *I*, has been theoretically predicted in the form $I = \left(1 + \frac{r}{a}\right)^{-10}$, where *a* is the average size of the field-enhancing feature and *r* is the distance of the analyte from the metal surface.
- The vibrational mode perpendicular to the surface are more enhanced than the other vibrational mode.

1.9 SER(R)S substrate

The most critical aspect of any SERS measurement is the substrate, that is responsible for the enhancement of the Raman signal. A given SERS substrate will exhibit a good enhancements in a limited excitation wavelength range: a SERS substrate excited at the wrong wavelength is no longer a SERS substrate (or only a really bad one). The location of the plasmon frequency in the electromagnetic spectrum is determined by the dielectric function, shape and size of the metal particle. The correlation between the silver nanoparticles absorbance spectrum and their size is reported in Figure 5. The absorbance spectra exhibit one or more peaks associated with the wavelength corresponding to the localized surface plasmon resonances of the substrate. Since SERS occurs precisely as a result of the interaction with such localized surface plasmon resonances, the largest SERS enhancement is expected when the incident laser is at a wavelength close to the plasmon wavelength.

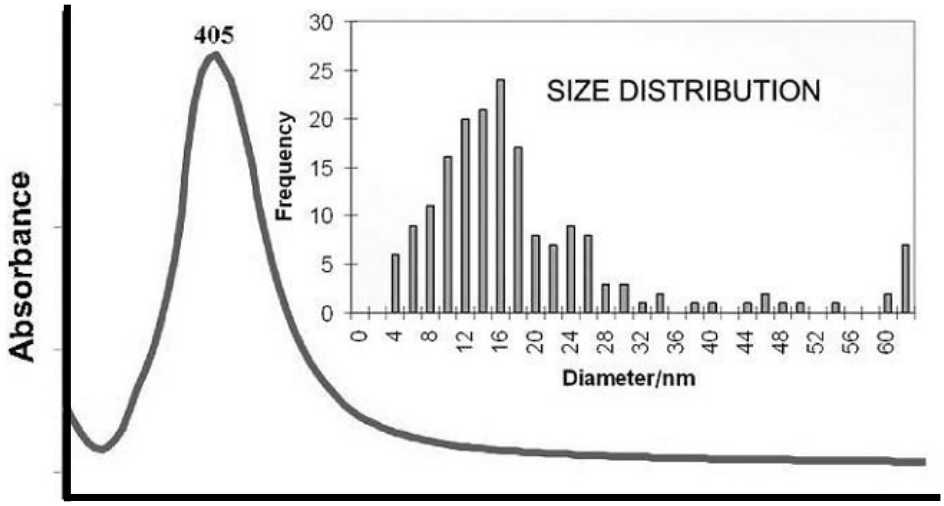

Figure 5: Absorbance spectrum of citrate reduced silver nanoparticles and size distribution of the nanoparticles (inset) [3].

Most SERS substrates are designed to operate with visible or near-infrared excitation (λ_{exc} = 400 ÷ 1000 nm), which is the typical range of interest for molecular Raman scattering experiments. In this range of frequencies gold or silver should be the metal of choice. Since the metal structure of a SERS-active substrate must be significantly smaller than the excitation wavelength, in this range of frequencies the dimensions are typically less than 100 nm.

SERS substrates can be tentatively classified into three main classes [12]:

- Metallic nanoparticles in suspension.
- "Planar" metallic structures, such as arrays of metallic nanoparticles supported on a planar substrate (glass, silicon, or metallic, for example).
- Metallic roughened electrodes.

Electrodes have played an important role in the historical development of SERS, including its discovery. Its importance has however been decreasing substantially,

mostly because of the relatively low enhancement factors typically achievable. One of the important applications of SERS is in the tracing of molecules in water, where silver and gold nanoparticles in suspension can provide the necessary SERS enhancements. Metal nanoparticles of different sizes and shapes have been synthesized using various methods, such as chemical reduction, chemical replacement, electrochemical reduction, photochemical, thermal decomposition, and ultrasonic decomposition methods. The simplest and the most widely used method is the chemical reduction method, in which a metal salt is reduced to metal nanoparticles in aqueous or non-aqueous solution by reducing agents. Normally some surfactants are to be added to the solution as capping agents to prevent the aggregation or oxidation of the synthesized nanoparticles or to adjust the growth rate of different facets to control the shape and size of the nanoparticles. The type of metal salt, reducing agent, surfactant, and their relative concentration, the reaction temperature, and the solution pH all influence the size and size distribution, the shape and the aggregation state of particles.

The methods to prepare highly ordered SERS substrates include the nanoparticle assembly method, the Langmuir-Blodgett method and nanolithography and nano-imprint methods.

The chemical assembly method is to modify a solid substrate with a bifunctional molecule. One of the functional group of the molecule interact with the solid substrate to form a monolayer, the other one interacts with the nanoparticles through electrostatic or chemical interaction to form an ordered layer of nanoparticles. The surface coverage and uniformity of the assembled layer depend primarily on the size, concentration, and surface charge of the nanoparticles, and the type of bifunctional molecules.

The Langmuir-Blodgett technique was originally used to prepare a large area film of amphiphilic molecules on solid substrates. To prepare a film, the nanoparticles should first be capped with a hydrophobic molecules and dispersed into highly volatile solvent (chloroform or hexane), which is immiscible with water. The nanoparticle suspension is dispersed onto the water surface and compressed into close-packed arrays by applying surface pressure. Emerging a solid substrate from the liquid a nanoparticles monolayer will be deposited homogeneously.

Another type of ordered SERS substrate that has been shown to be very promising is fabricated on the basis of the nanosphere lithography method, by assembly of polystyrene or silica spheres of desired size on a clean substrate. The nanosphere assembly is then used as the template for vacuum deposition or electrochemical deposition to form on the template a metal film of the desired thickness. As a result, three kinds of structured SERS substrates may be produced: (1) physical vapor deposition on the nanosphere template leads to the formation of a metal "film over nanosphere" surface; (2) removal of nanospheres after the metal formation results in surface-confined nanoparticles with a triangular footprint; (3) electrochemical deposition followed by removal of the nanosphere leaves a thin nanostructured film containing a regular hexagonal array of a uniform metal nanoisland.

To obtain a highly ordered array nanolithography or nanoimprint method should be used. Typically, a layer of polymeric photoresist is cast on the solid substrate, followed by patterning with light. After exposure and development, the remaining photoresist can be used as a mold, on which SERS-active metals are deposited. After the mold has been lifted off, a highly ordered nanostructured SERS-

active substrate with a structure identical or complementary to that of the mold is formed.

With the Langmuir-Blodgett, nanolithography and nano-imprint methods the shape, size, and spacing of the nanostructures can be controlled precisely, so that the LSPR position can be adjusted to match the excitation wavelength and to achieve an optimized SERS enhancement. The procedures complexity and the requirement of specific equipment reduce the applicability of those techniques.

1.10 References

[1] G. Smith e E. Dent, Modern Raman spectroscopy: a practical approach., Chichester, U.K.: John Wiley and Sons, 2005.

[2] G. Turrel e J. Corset, Raman Microscopy Developments and Applications, San Diego: Elsevier - Academic Press, 1996.

[3] R. Aroca, Surface enhanced vibrational spectroscopy., Chichester, U.K.: John Wiley and Sons, 2006.

[4] J. A. Dieringer Wustholz, K. L. Wustholz, D. J. Masiello, J. P. Camden, S. L. Kleinman, G. C. Schatz e R. P. Van Duyne, «Surface-enhanced Raman excitation spectroscopy of a single rhodamine 6G molecule,» *J. Am. Chem. Soc,* vol. 131, pp. 849-854, 2009.

[5] P. Hildebrandt e M. Stockburger, «Surface-enhanced resonance Raman spectroscopy of Rhodamine 6G adsorbed on colloidal silver,» *The Journal of Physical Chemistry,*, vol. 88, pp. 5935-5944., 1984.

[6] I. Chourpa, F. H. Lei, P. Dubois, M. Manfait e G. D. Sockalingum, «Intracellular

applications of analytical SERS spectroscopy and multispectral imaging,» *Chem. Soc. Rev,* vol. 37, pp. 993-1000, 2008.

[7] E. Arceo, R. A. Alvarez-Puebla, P. J. G. Goulet, J. J. Garrido e R. F. Aroca, «Role of Nanoparticle Surface Charge in Surface-Enhanced Raman Scattering,» *J. Phys. Chem. B,* vol. 109, pp. 3787-3792, 2005.

[8] P. C. Lee e D. Meisel, «Adsorption and surface-enhanced Raman of dyes on silver and gold sols Adsorption and Surface-Enhanced Raman of Dyes on Silver and Gold Sols,» *J. of Phys. Chem.,* vol. 86, pp. 3391-3395, 1982.

[9] Larmour, K. Faulds e D. Graham, «SERS activity and stability of the most frequently used silver colloids,» *J.Raman Spectrosc,* vol. 43, pp. 202-206, 2012.

[10] H. Munro, W. E. Smith, M. Garner, J. Clarkson e P. C. White, «H. Munro, W. E. Smith,Characterization of the Surface of a Citrate-Reduced Colloid Optimized for Use as a Substrate for Surface-Enhanced Resonance Raman Scatterin,» *Langmuir,* vol. 11, pp. 3712-3720, 1995.

[11] N. Leopold e B. Lendl, «A New Method for Fast Preparation of Highly Surface-Enhanced Raman Scattering (SERS) Active Silver Colloids at Room Temperature by Reduction of Silver Nitrate with Hydroxylamine Hydrochloride,» *J. Phys. Chem. B,* vol. 107, pp. 5723-5727, 2003.

[12] E. C. Le Ru e P. G. Etchegoin, Principles of Surface Enhanced Raman Spectroscopy and related plasmonic effects, Oxford: Elsevier, 2009.

[13] E. Smith e G. Dent, Modern Raman spectroscopy - A practical approach, West Sussex: John Wiley & Sons Ltd, 2005.

[14] J. R. Ferraro e K. Nakamoto, Introductory Raman spectroscopy, Academic Press, 2003.

[15] H. Ko, S. Singamaneni e V. V. Tsukruk, «Nanostructured surfaces and assemblies as SERS media,» *Small,* vol. 4, pp. 1576-1599, 2008.

[16] E. C. Le Ru e P. G. Etchegoin, Principles of Surface Enhanced Raman Spectroscopy and related plasmonic effects, Oxford, 2009: Elsevier, 2009.

Chapter 2:

Introduction to SERRS substrate for bilirubin detection and quantification

In this chapter and following the development and implementation of coated silver nanoparticles to measure the anionic chromophore bilirubin is reported.

A high affinity of the analyte for the metal substrate of choice is an essential requirement for obtaining a SERS signal. In many cases, the interaction between the analyte and the metal surface is mediated by electrostatic forces operating between opposite charges, in addition to more specific interactions. One of the most used protocol to prepare Ag nanoparticles for SERS is the reduction of Ag+ ions with sodium citrate [1, 2]. The nanoparticles have a negative surface charge due to the adsorbed citrate anions [3], so that this substrate provides a poor SERS enhancement when used with negatively-charged analytes. The same problem is encountered when using hydroxylamine as reducing agent, which yields negatively charged colloids [2, 4]. To overcome this problem, other synthetic methods have been developed in which different reducing agents are used [2, 5]. Reduction with NaBH4 yields positively charged Ag nanoparticles, but these colloids are less stable than citrate- reduced ones [2, 3, 6]. Another strategy consists in coating Ag nanoparticles with a layer of

positively charged molecules, such as silanes [7], cetyltrimethylammonium bromide (CTAB) [8] and polyethyleneimine [9].

In chapter 3 and chapter 4 the development of a SE(R)RS-substrate consisting of Ag nanoparticles with a positive surface charge to be used for the analysis of bilirubin is described. The organic anions can be adsorbed on the SERS substrate via electrostatic interaction, and can thus be detected using SE(R)RS. Since bilirubin is considered itself hydrophobic [10], due to the presence of many hydrophobic groups [11], in chapter 5 a substrate for detecting bilirubin consisting of Ag nanoparticles with an hydrophobic capping is proposed. In this chapter a brief description of bilirubin is reported.

The bilirubin is a yellow organic molecule of clinical interest formed as a metabolic waste product of heme breakdown [10, 12-14].

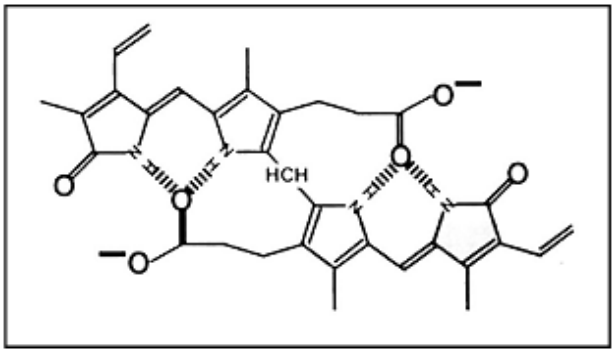

Figure 6: Bi-dimensional scheme of the di-anionic form of bilirubin [13]

Due to the presence of the two propionic acid chains in aqueous solutions bilirubin is thought to be mainly present as a di-anion [13] (Figure 6). But bilirubin preferentially adopts an intramolecularly hydrogen –bonded ridge - tile conformation (Figure 7), which explains its surprising lipophilicity. Free bilirubin is extremely

apolar and practically insoluble in water at physiologic pH and temperature (pH 7.4 and 37 °C) [15].

The free bilirubin is carried by albumin to the liver. In the liver it is conjugated with glucuronic acid by the enzyme glucuronyl-transferase, making it soluble in water. Once it is conjugated, bilirubin can be excreted in the urin. Hence in serum, the bilirubin is found either conjugated with glucuronic acid or in its unconjugated form (bonded to albumin), whereas very little bilirubin is thought to exists as "free" (i.e. un-bound and un-conjugated).

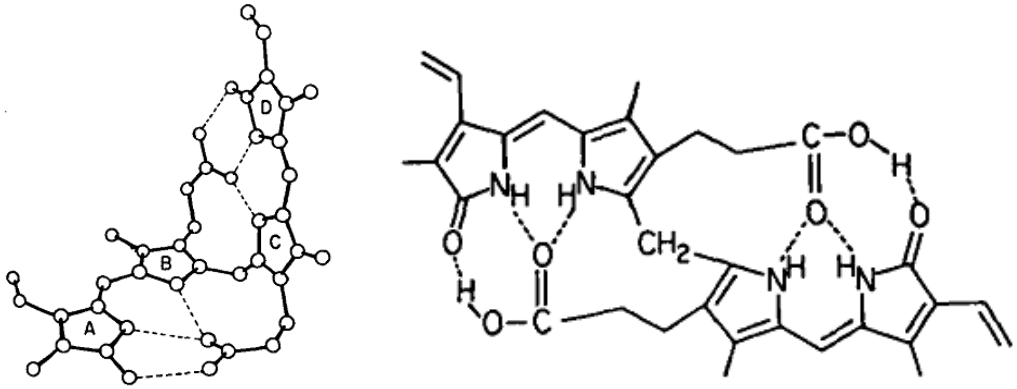

Figure 7: Structure of free bilirubin. The intra-molecularly hydrogen –bonded ridge - tile conformation, with hydrogen bonds represented by dotted lines (right) and the equivalent structure in simplified planar form [10**].**

The free form is toxic, as it can cross the blood-brain barrier and damage the brain (kernicterus) [16]. In clinical practice the total amount of bilirubin is used as an easily measured proxy for the concentration of free bilirubin; however, this indirect gross estimation can be inadequate for evaluating the risk of kernicterus.

The only currently available method for free bilirubin quantification relies on the measurement of the decrease in bilirubin absorbance due to a selective enzymatic oxidation of free bilirubin in diluted serum (i.e. "peroxidase method") [17, 18].

However, the equilibrium between free- and albumin-bound bilirubin seem to be heavily influenced by dilution issues, so that the "peroxidase method" leads to widely varying results, raising serious concerns about the reliability of this method [23]. Hence, alternative methods for bilirubin quantification are highly desirable.

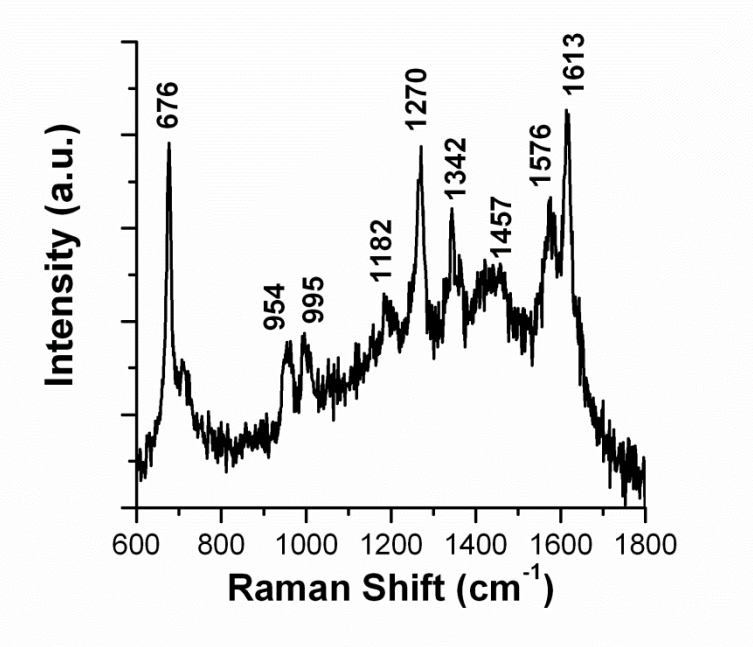

Figure 8: Resonance Raman spectrum of bilirubin 100 μM. λ_{exc}=514 nm, 7 mW, 30s.

Despite several works reporting RR spectra of bilirubin solutions in a variety of solvents and conditions [20-24], there is a lack of published studies about the application of SERRS to bilirubin [25,26] and in particular to bilirubin detection [27]. Figure 8 shows a resonance Raman spectrum of bilirubin.

According to previous studies on the RR spectrum of bilirubin [22,24], the bands at 1576 and 1613 cm^{-1} of the bilirubin RR spectrum (Figure 8) originate from C=C, C=O, and C−N stretching modes of the lactam rings, whereas the band at 1270 cm^{-1} is due to a lactam ring C−C stretching and N−H bending modes. On the other

hand, the assignment of many other bands, such as those at 954 and at 676 cm^{-1}, is still uncertain.

2.1 References

[1] P C Lee and D Meisel, "Adsorption and surface-enhanced Raman of dyes on silver and gold sols Adsorption and Surface-Enhanced Raman of Dyes on Silver and Gold Sols," *J. of Phys. Chem.*, vol. 86, pp. 3391-3395, 1982.

[2] Larmour, K Faulds, and D Graham, "SERS activity and stability of the most frequently used silver colloids," *J.Raman Spectrosc*, vol. 43, pp. 202-206, 2012.

[3] H Munro, W E Smith, M Garner, J Clarkson, and P C White, "H. Munro, W. E. Smith,Characterization of the Surface of a Citrate-Reduced Colloid Optimized for Use as a Substrate for Surface-Enhanced Resonance Raman Scatterin," *Langmuir*, vol. 11, pp. 3712-3720, 1995.

[4] N Leopold and B Lendl, "A New Method for Fast Preparation of Highly Surface-Enhanced Raman Scattering (SERS) Active Silver Colloids at Room Temperature by Reduction of Silver Nitrate with Hydroxylamine Hydrochloride," *J. Phys. Chem. B*, vol. 107, pp. 5723-5727, 2003.

[5] R A Alvarez-Puebla and R F Aroca, "Synthesis of Silver Nanoparticles with Controllable Surface Charge and Their Application to Surface-Enhanced Raman Scattering," *Anal.Chem*, vol. 81, pp. 2280-2285, 2009.

[6] E C Le Ru and P G Etchegoin, *Principles of Surface Enhanced Raman Spectroscopy and related plasmonic effects*. Oxford: Elsevier, 2009.

[7] S M Ngola, J Zhang, B L Mitchell, and N Sundararajan, "Strategy for improved

analysis of peptides by surface-enhanced Raman spectroscopy (SERS) involving positively charged nanoparticles," *J. Raman Spectrosc.*, vol. 39, pp. 611–617, 2008.

[8] Z Sui et al., "Capping effect of CTAB on positively charged Ag nanoparticles," *Physica E: Low-dimensional Systems and Nanostructures*, vol. 33, pp. 308-314, 2006.

[9] S Sanchez-Cortes, R M Berenguel, A Madejon, and M Perez-Mendez, "Adsorption of Polyethyleneimine on Silver Nanoparticles and Its Interaction with a Plasmid DNA: A Surface-Enhanced Raman Scattering Study," *Biomacromolecule*, vol. 3, pp. 655-660, 2002.

[10] B T Doumas and T W Wu, "The measurement of bilirubin fractions in serum," *Critical reviews in clinical laboratory sciences*, vol. 28, pp. 415-445, 1991.

[11] J D Ostrow, P Mukerjee, and C Tiribelli, "Structure and binding of unconjugated bilirubin: relevance for physiological and pathophysiological function," *Journal of Lipid Research*, vol. 35, pp. 1715 - 1737, 1994.

[12] J D Ostrow, *Bile pigments and jaundice: molecular, metabolic, and medical aspects*.: Dekker, 1986.

[13] J D Ostrow, P Mukerjee, and Claudio Tiribelli, "Structure and binding of unconjugated bilirubin: Relevance for physiological and pathophysiological function," *Journal of lipid research*, vol. 35, pp. 1715-1737, 1994.

[14] M J Maisels and A F McDonagh, "Phototherapy for neonatal jaundice," *The New England journal of medicine*, vol. 358, pp. 920-928, 2008.

[15] R Brodersen, "Bilirubin: solubility and interaction with albumin and phospholipid," *J.Biol.Chem*, vol. 254, pp. 2364 - 2369, 1979.

[16] R P Wennberg, C E Ahlfors, V K Bhutani, L H Johnson, and S M Shapiro, *Pediatrics*, vol. 117, pp. 130-135, 2006.

[17] C E Ahlfors, "Measurement of Plasma Unbound Unconjugated Bilirubin ," *Analytical biochemistry*, vol. 279, pp. 130-135, 2000.

[18] J Jacobsen and R P Wennberg, "Determination of Unbound Bilirubin in the Serum of Newborns," *Clin. Chem*, vol. 20, pp. 783-789, 1974.

[19] J M Kirk, "Neonatal jaundice: a critical review of the role and practice of bilirubin analysis," *Annals of clinical biochemistry*, vol. 45, pp. 452-462, 2008.

[20] Y Z Hsieh and M D Morris, "Resonance Raman spectroscopic study of bilirubin hydrogen bonding in solutions and in the albumin complex," *Journal of the American Chemical Society*, vol. 110, pp. 62-67, 1988.

[21] L Margulies and M Toporowicz, "Resonance raman and electronic absorption spectroscopy of bilirubin in solution. An experimental and theoretical study," *Journal of Molecular Structure*, vol. 174, pp. 153-158, 1988.

[22] B Yang, M D Morris, M Xie, and D A Lightner, "Resonance Raman spectroscopy of bilirubins: Band assignments and application to bilirubin/lipid complexation," *Biochemistry*, vol. 30, pp. 688-694, 1991.

[23] E Hu, F Liang, Duschek, and W Kiefer, "Resonance Raman spectroscopic study of free brilirubin and brilirubin complexes with copper(II), silver(I) and gold(III)," *Spectrochimica Acta Part A: Molecular and Biomolecular Spectroscopy*, vol. 53, pp. 1431-1438., 1997.

[24] J Yin and H Watarai, "Resonance raman spectroscopic study on chiral aggregation of bilirubin-bovine serum albumin complex formed at liquid/liquid interface," *Analytical sciences: the international journal of the Japan Society for Analytical Chemistry*, vol. 23, pp. 841-846, 2007.

[25] Y Z Hsieh, N S Lee, R S Sheng, and M D Morris, "Surface-enhanced Raman

spectroscopy of free and complexed bilirubin," *Langmuir,* vol. 3, pp. 1141-1146, 1987.

[26] J Chen, J Hu, Z Xu, and R S Sheng, "Surface-enhanced Raman spectroscopy of free bilirubin and bilirubin complexes with transition metals iron(II), nickel(II) and cobalt(II)," *Spectrochimica Acta Part A: Molecular Spectroscopy*, vol. 50, pp. 929-936, 1994.

[27] R Sulk et al., "Surface-enhanced Raman assays (SERA): Measurement of bilirubin and salicylate," *Journal of Raman Spectroscopy*, vol. 30, pp. 853-859, 1999.

Chapter 3:

Poly-L-lysine coated silver nanoparticles as positively charged substrates for bilirubin detection[1]

3.1 Introduction

In this chapter the development of a SE(R)RS-substrate consisting of Ag nanoparticles with a positive surface charge to be used for the analysis of bilirubin will be described. The organic anions can adsorb on the SERS substrate via electrostatic interaction, and can thus be detected using SE(R)RS.

The Ag nanoparticles with a positive surface charge was obtained upon coating citrate-reduced Ag nanoparticles (Cit-AgNPs), a widely used substrate because of its ease of preparation and efficient enhancement of Raman spectra [1], with poly-L-lysine (PLL). PLL is a small natural homopolymer belonging to the group of cationic

[1] Adapted from Marsich L, Bonifacio A, Mandal S, Krol S, Beleites C, and Sergo V, "Poly-L-lysine coated silver nanoparticles as positively charged substrates for Surface Enhanced Raman Scattering", Langmuir, 2012, 28, 13166−13171.

poly-amino acids, and even in moderately alkaline media it contains positively charged hydrophilic amino groups (pKa=10,53). In this chapter the preparation of PLL-coated Ag nanoparticles (PLL-AgNPs) and their characterization using UV-Vis spectrophotometry, transmission electron microscopy, dynamic light scattering (DLS), zeta (ζ) potential measurements and SERS spectroscopy were reported.

The application of the PLL-AgNPs as SERRS sensors for bilirubin quantification is also presented, in particular a calibration curve was done, confidence bands were calculated with the purpose of quantifying bilirubin in samples with unknown concentration. As reported in chapter 2.0, at physiological pH, in aqueous solutions bilirubin is thought to be mainly present as a di-anion [2].

As also said in chapter 2, despite several works reporting RR spectra of bilirubin solutions [3-7], there is a lack of published studies about the application of SERRS to bilirubin [8,9] and in particular to bilirubin detection [10]. This scarcity could be possibly due to the lack of a reliable positively-charged SERS-active metal colloid having a high affinity for the bilirubin anions.

The PLL-AgNPs described in this chapter were shown to be an efficient SERRS substrate for bilirubin quantification in buffer solutions.

3.2 Experimental section

3.2.1 Materials

Silver Nitrate ($AgNO_3$), dimethyl sulfoxide (DMSO), sodium citrate tribasic dehydrate, poly-L-lysine hydro-bromide (PLL) (mol wt 15,000-30,000), bilirubin (mixture of isomers (IIIA, VIIIA and IXA)) and sodium hydroxide were purchased from Sigma-Aldrich.

Phosphate buffer solution (20 mM, pH 8.00) was prepared using K_2HPO_4 and KH_2PO_4, both purchased from Sigma-Aldrich. All chemicals were used without further purification.

Ultra pure Milli-Q water (Merck Millipore, Billerica, MA, USA) was used for the preparation of all solutions.

3.2.2 *Cit-AgNPs preparation*

Cit-AgNPs were prepared according to the procedure described by Lee and Meisel [11]. 45 mg of $AgNO_3$ were dissolved in 250 mL of Milli-Q water. The solution was heated to boiling under reflux, and then 5 mL of freshly prepared tri-sodium citrate aqueous solution (1% w/v) was added drop wise under vigorous stirring. The mixture was kept boiling under reflux and stirring for 1 h and then slowly cooled down to room temperature.

All glassware was thoroughly cleaned using concentrated HNO_3 and then chromic acid (2.77 g $K_2Cr_2O_7$ in 100 mL H_2SO_4), and carefully rinsed with Milli-Q water.

3.2.3 *Poly-L-lysine coated silver nanoparticles (PLL-AgNPs) preparation*

A 0.1% w/v poly-L-lysine aqueous solution was prepared. Then, 50 mL of this PLL solution were added to 50 mL of Cit-AgNPs previously diluted 1:25 with Milli-Q water. In order to remove PLL excess, the mixture was centrifuged in 1.5 mL polypropylene eppendorf tubes at 6708 × g for 20 minutes, the supernatant was removed and fresh Milli-Q water was added. This washing procedure was repeated 3 times. The resulting coated-nanoparticles dispersion is stable against aggregation for up 24 h.

Before its use as SERS substrate, the stock dispersion of coated nanoparticles was pelleted by centrifugation and removal from each eppendorf tube of 1.47 mL of the supernatant (corresponding to 98% of the initial volume) with a micropipette, resulting in a concentrated aqueous dispersion of coated nanoparticles.

3.2.4 Nanoparticles characterization

UV-Vis spectra were acquired with a Perkin Elmer Lambda bio20 spectrophotometer, between 350 nm and 700 nm. Samples were prepared by diluting 10× the citrate-reduced silver nanoparticles stock solution with Milli-Q water in a 3 mL cuvette.

DLS and the ζ-potential measurements were performed using a Malvern Instruments' Zetasizer (Nano-ZS Nanoseries, UK).

Transmission electron microscopy (TEM) was performed with a Philips EM208 scanning electron microscope using a carbon coated nickel grid (Carbon Film 200 Mesh, Ni, 50/bx produced by Electron Microscopy Sciences). Uranyl acetate ($UO_2(CH_3COO)_2 \bullet 2H_2O$) was added to the dried PLL-AgNPs on the TEM grids as contrast agent, to visualize the positively charged organic layer around the NPs, as reported in literature for the chitosan [12].

3.2.5 Raman instrumentation

Spectroscopic measurements were done using an inVia Raman system (Renishaw, Wotton-under-Edge, UK). The laser sources (514.5 nm argon-ion laser and 785 nm diode laser) were focused on the sample, consisting of a 50 μL drop deposited on a UV-grade CaF_2 slide, through a 10× objective (0.25 N.A.).

The 514.5 nm and 785 nm laser power at the sample was 7 mW and 150 mW, respectively, except for bilirubin SERRS measurement, in which case the power of the 514.5 nm laser was 650 μW to avoid bilirubin photodegradation. To avoid interference from anomalous bands arising from Ag colloids when green excitation is used [13], SERS spectra of PLL-AgNPs were obtained using the 785 nm laser.

3.2.6 Bilirubin solutions

A bilirubin stock solution was prepared dissolving bilirubin in anhydrous dimethyl sulfoxide to obtain a final concentration of 5 mM. 100 μM bilirubin solutions were prepared diluting 50 times the stock solution with a 10 mM NaOH aqueous solution. Solutions with a bilirubin concentration lower than 100 μM were prepared using a 20 mM buffer phosphate solution (pH 8) for dilution. Extreme care was taken to avoid bilirubin photodegradation upon light exposure: all dilutions were done in a dark room with red safelight illumination.

Normal-Raman spectrum of citrate aqueous solution with 1 M concentration was acquired using the 514.5 nm laser with an acquisition time of 50 s. Cit-AgNPs SERS spectrum was collected using the 514.5 nm with a total acquisition time of 30 s.

The normal Raman spectrum of solid PLL was acquired with a 785 nm laser and the acquisition time was 10 s. 100 μM bilirubin RR spectra were collected using the 514.5 nm laser with an acquisition time of 30 s. SERRS spectra of bilirubin were collected with the 514.5 nm laser adding 2,5 μL of the PLL-AgNPs to 50 μL of bilirubin solution with an acquisition time of 50 s.

For each bilirubin concentration, three different bilirubin solutions were prepared and measured independently. Extreme care was taken to avoid bilirubin photodegradation upon laser exposure.

3.2.7 *Data processing*

All data pre-processing and analysis was performed using several packages of the R software for statistical analysis [14]. The position of the bands was estimated with msProcess [15], a package providing tools for spectra processing. Raman and SERS spectra were analyzed with hyperSpec [16], an R package to handle hyperspectral data sets, in this case spectra plus concentrations.

For bilirubin quantification, the region between 600 cm^{-1} and 800 cm^{-1} of the spectra was considered, since in this region of the spectrum the PLL does not have any interfering band. A linear baseline correction was performed. The intensity at the maximum of the 680 cm^{-1} band of the bilirubin SERRS spectrum was chosen for calibration purposes.

The calibration curve, the 95% confidence interval for the calibration, the limit of detection (LOD) and the limit of quantification (LOQ) were calculated using chemCal [17], an R package for calibration data in analytical chemistry. The use of weighted regression for calibration was considered and checked, but it was found not necessary, as the standard deviation of SERS intensity was not increasing with concentration in the interval used for calibration.

3.3 Results and discussion

3.3.1 *Nanoparticles characterization*

The Cit-AgNPs have an absorption maximum at 405 nm (Figure 9), indicating that the average diameter of the nanoparticles is between 70 and 80 nm, as reported in literature [18], [19], [11]. The PLL-AgNPs have an absorption maximum at 410 nm (Figure 9). This red shift of the plasmonic frequency from 405 to 410 nm can be

attributed to the adsorption of the PLL on the nanoparticles surface, indicating that the coating succeeded.

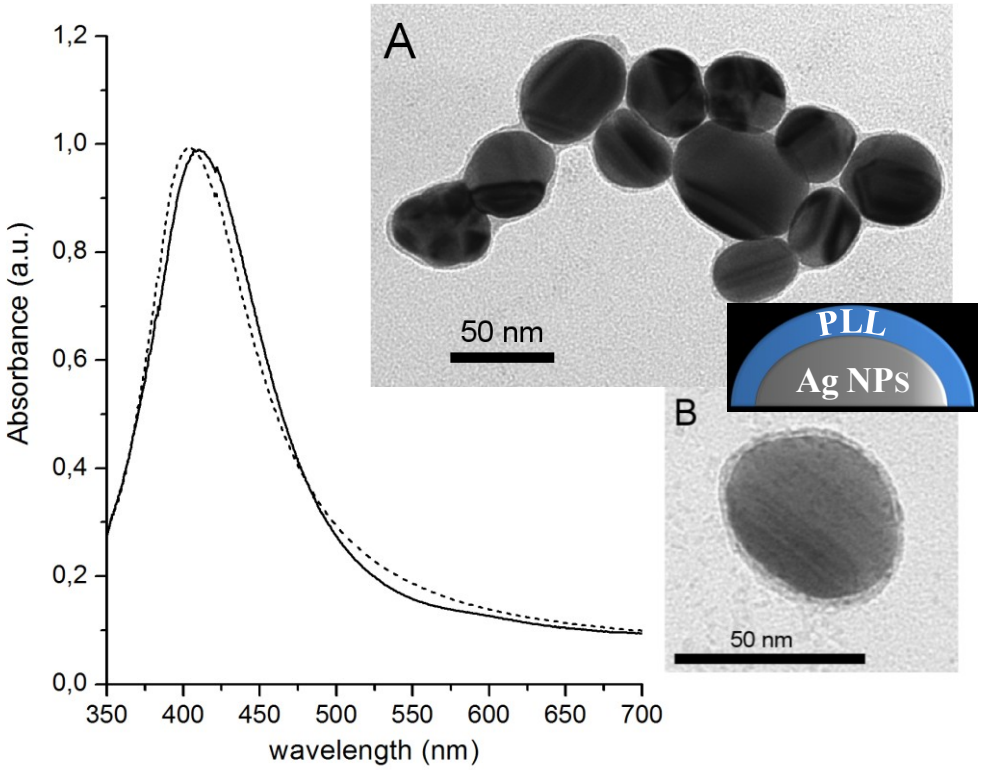

Figure 9: UV-vis extinction spectra of Cit-AgNPs (dashed line) and PLL-AgNPs (solid line); TEM images (insets A, B) of PLL-AgNPs (treated with uranyl acetate $UO_2(CH_3COO)_2 \bullet 2H_2O$) to enhance the contrast due to the PLL layer around the AgNPs) and C) a schematic representation of the PLL layer around the nanoparticles.

The relatively small 5 nm red shift rules out the formation of large nanoparticles aggregates upon PLL coating TEM images of the PLL-AgNPs (Figure 9: UV-vis extinction spectra of Cit-AgNPs (dashed line) and PLL-AgNPs (solid line); TEM images (insets A, B) of PLL-AgNPs (treated with uranyl acetate $UO_2(CH_3COO)_2 \bullet 2H_2O$) to enhance the contrast due to the PLL layer around the AgNPs, insets) confirm the size of the NPs as determined with UV-Vis spectrophotometry and the negative stain with uranyl acetate clearly shows the PLL

layer around the nanoparticles. The ζ-potentials of the Cit-AgNPs and of the PLL-AgNPs are -35.0 ± 1.2 mV and +62.3 ± 1.64 mV, respectively, confirming the modification of the nanoparticles surface charge from negative to positive upon PLL coating. Furthermore, ζ-potential absolute values are greater than 30 mV, indicating that the suspension of Cit-AgNPs and PLL-AgNPs in water are stable [20]. The ζ-potential for the PLL-AgNPs is more positive than those reported in literature for other SERS-active coated nanoparticles [21, 22], indicating a greater charge density and therefore potentially electrostatic interactions with negatively charged analytes. The values of the average hydrodynamic diameter, measured with DLS, are 92.9 ± 1.7 nm for the Cit-AgNPs and 86.4 ± 1.1 nm for the PLL-AgNPs. The negligible difference between these two values, possibly caused by the different charge density at the surface, confirms that no aggregation occurs during the coating process.

The normal-Raman spectrum of citrate aqueous solution and the SERS spectrum of the Cit-AgNPs (Figure 10 a and b) show intense vibrational bands between 800 and 1050 cm^{-1} and between 1300 and 1450 cm^{-1}, in agreement with the data previously reported in literature [1]. The presence of the same spectral features in both Raman and SERS spectra demonstrates that citrate ions are adsorbed on the silver nanoparticles. According to literature [1], the bands between 1300 cm^{-1} and 1500 cm^{-1} are due to symmetric carboxylate stretching mode and those between 800 cm^{-1} and 1000 cm^{-1} are caused by C-COO and C-OH stretching modes. The relative band intensities in SERS spectra are governed by the orientation of the molecules adsorbed on the metal surface (i.e. SERS selection rules) [23], and they suggest that citrate ions adsorb to the Ag surface through their carboxylic groups, as proposed by Munro et al. [1].

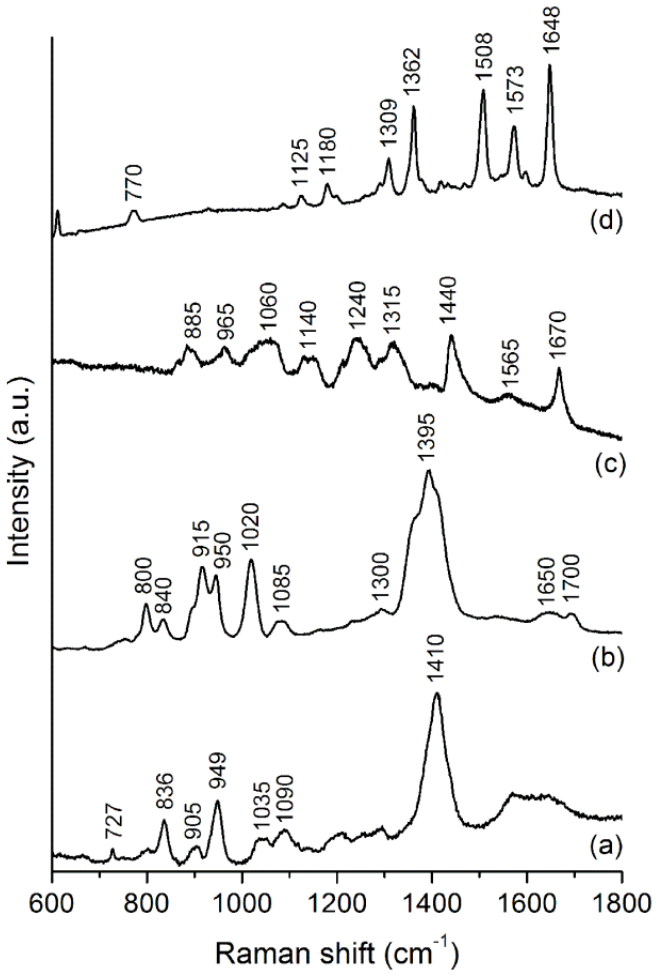

Figure 10: (a) Raman spectrum of 1 M citrate solution; (b) SERS spectrum of Cit-AgNPs; (c) Raman spectrum of PLL; (d) SERS spectrum of PLL-AgNPs. λ_{ex} is 514.5 nm for (a), (b), (d) and 785 nm for (c).

On the other hand, the SERS spectrum of the PLL-AgNPs (Figure 10d) does not show the citrate spectral features, but exhibits several bands that are also found in the Raman spectrum of the PLL (Figure 10c). In particular, the bands at 1678 and 1240 cm^{-1} in the SERS spectrum of PLL-AgNPs were assigned to the amide I and amide III modes, respectively, observed at similar Raman shifts in the PLL Raman spectrum. Such values for these amide modes indicate that the "random coil" structure of the PLL in aqueous solution has been retained upon adsorption on the metal surface [24].

Beside the amide I and III, other bands in the SERS spectrum of Figure 10d can be attributed to PLL, most notably the ones at 1440, 1132, and around 890 cm^{-1}. The observation of such bands is consistent with the displacement of citrate by PLL on the nanoparticles surface, corroborating the conclusions inferred from UV−vis, TEM, and ζ-potential measurements.

The interpretation of the PLL-AgNPs in terms of detailed adsorption geometry is not trivial, and it is further complicated by the presence of other bands apparently absent in the PLL Raman spectrum. For instance, the sharp band at 1003 cm^{-1} is probably due to residual aromatic protecting group used in the PLL synthesis (as described by PLL purveyor). Amino groups are known to strongly interact with Ag, [25] and such an interaction in the case of PLL on Ag is supported by the presence of the bands at 1132 and 1034 cm^{-1} (Figure 10d), both of which have been associated with vibrations of the amino group in SERS spectra of amines [26].

3.3.2 SERRS spectra of bilirubin

Spectra of a 100 nM bilirubin solution with (Figure 11a) and without (Figure 11b) the Cit-AgNPs does not show any detectable vibrational band. On the contrary, the same bilirubin solution measured in the presence of PLL-AgNPs (Figure 10c) yields an intense SERRS spectrum, showing the same features as those of the RR spectrum of a concentrated (100 μM) bilirubin solution (Figure 12b). Indeed, the wavelength of laser used for Raman excitation (i.e. 514.5 nm) is in resonance with an electronic transition of bilirubin, allowing the coupling of SERS with RR to yield a SERRS spectrum. Both SERRS and RR spectra of bilirubin are consistent with those previously reported Figure 11c and Figure 12 [21-28]. The band assignment for the RR spectrum is reported in chapter 2.1.

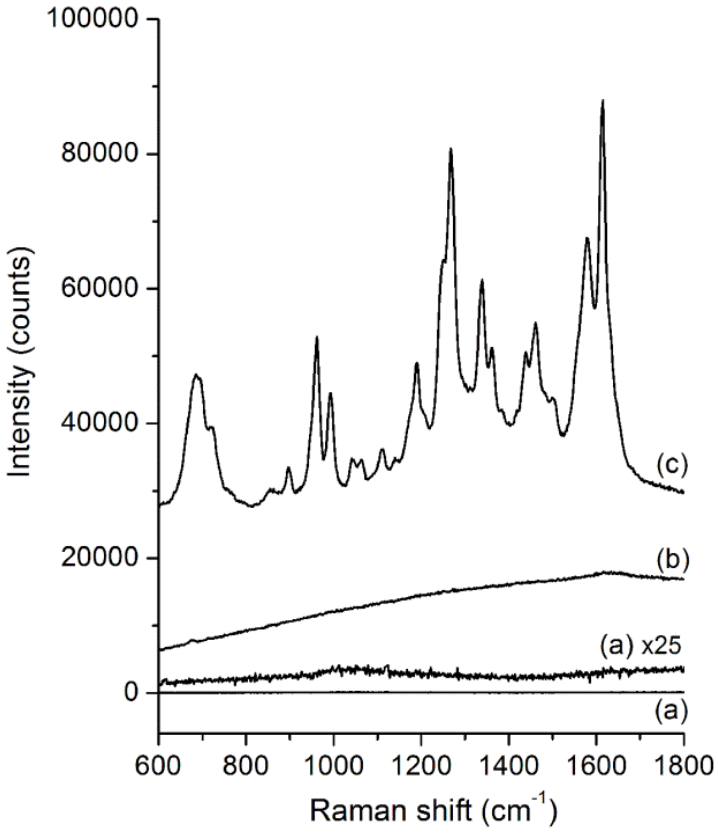

Figure 11: (a) Raman spectrum of 100 nM bilirubin with Cit-AgNPs; (b) Raman spectrum of 100 nM bilirubin; (c) SERRS spectrum of 100 nM bilirubin with PLL-AgNPs; all the spectra are shown on the same intensity scale; because of its low intensity, spectrum (a) magnified 25 times (x25) is also reported; λ_{ex} = 514.5 nm.

The bilirubin SERRS spectrum (Figure 12a) is very similar to the RR spectrum (Figure 12b), and therefore its bands can be readily assigned according to the same scheme. This similarity in the relative intensity pattern between RR and SERRS spectra is expected, and it is due to a relaxation of the SERS surface selection rules in the resonant conditions present in SERRS [18, 27].

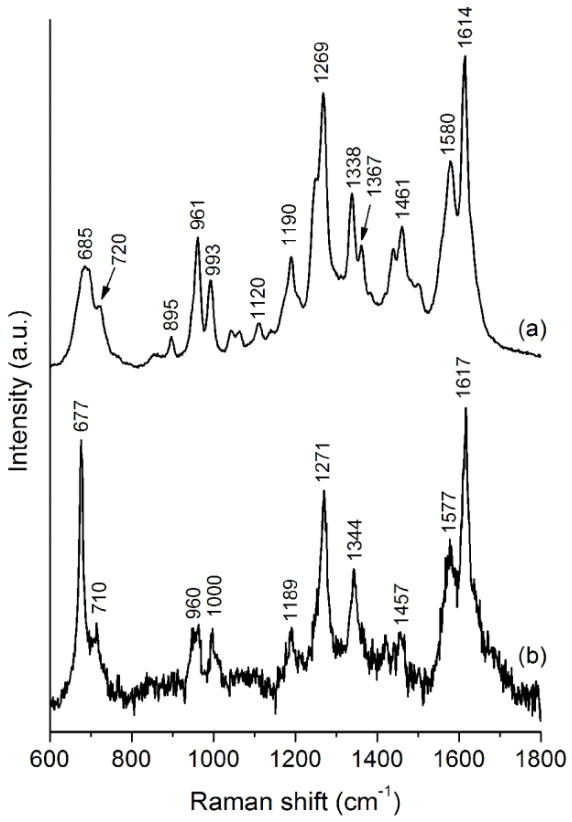

Figure 12: Comparison between (a) 100 nM bilirubin SERRS spectrum and (b) 100 μM bilirubin RR spectrum; intensity of both stacked spectra was normalized for better comparison; λ_{ex} = 514.5 nm.

The small shifts (< 3–4 cm^{-1}) observed between most bands of RR and SERRS spectra suggest that the bilirubin intramolecular hydrogen-bonding pattern between carboxylates and pyrrolic hydrogens is, at least in part, still present, [3,5] although altered upon adsorption. Similar changes in some of the hydrogen-bonding sensitive bands, such the small down shift for the 1617 cm^{-1} and the 1271 cm^{-1} bands, and the up shift of the 1577 cm^{-1} band, were also observed in the RR spectrum of bilirubin–albumin complex, [3] suggesting a parallel with PLL–bilirubin. When complexed with albumin, bilirubin forms salt-bridges between its carboxylates and two charged amino-acidic amino-groups of the protein, while maintaining one intra-

molecular hydrogen bond between a carboxylate and two pyrrolichydrogens [28]. At the same time, one of the lactam carbonyls becomes loosely hydrogen bonded to the protein.

A similar interaction could reasonably take place also between bilirubin and PLL-AgNPs, because PLL has positively charged amino groups and can act as a hydrogen-bond donor to the bilirubin lactam carbonyls. Unfortunately, a direct proof about salt-bridges formation from RR/SERRS spectra is not possible, because propionates carboxylates are not conjugated with the extended chromophoric π-systems of bilirubin, and therefore do not benefit from the RR enhancement, remaining undetected in resonant spectra. However, indirect effects of such interaction can be observed. A loosening of the intramolecular hydrogen bonds due to the formation of salt- bridges between carboxylates could explain the down shift of the N−H bending mode, whereas the formation of a weak hydrogen bond between PLL and one of the lactam carbonyls could explain the upshift of the mode at 1617 cm^{-1}, associated with a lactam carbonyl stretching. The up shift the other lactam mode at 1577 cm^{-1}, and the upshift and dramatic broadening of the sharp and intense unassigned band at 677 cm^{-1}, are more difficult to explain. In general, a more detailed description of the PLL−bilirubin interaction, which is beyond the scope of this Article, would require a more comprehensive and consistent bilirubin normal-mode analysis.

The dominant contribution of the resonance effect to the SERRS spectrum allows the detection of the bilirubin even if it is not directly adsorbed on the metal surface, but on the top of the PLL coating. On the other hand, the PLL coating does not benefit from the resonance enhancement, and its SERS spectrum is less intense than the SERRS spectrum of bilirubin, but still observable in the absence of bilirubin (Figure 10d).

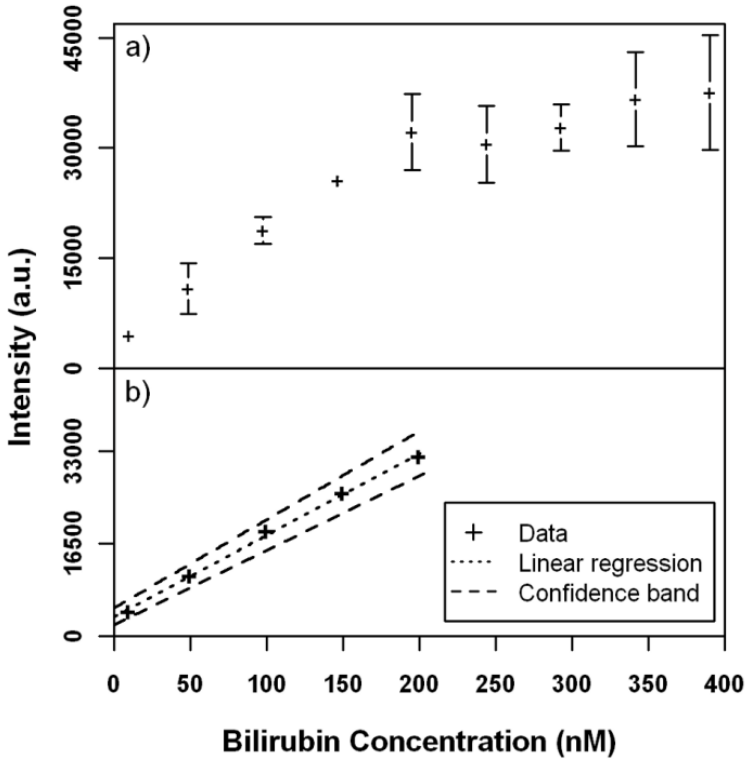

Figure 13: a) Bilirubin SERRS intensities at 690 cm^{-1} as a function of bilirubin concentration. b) Intensity average value of the band at 690 cm^{-1} (crosses), calibration curve in the concentration range 10 – 200 nM (dotted line) and the 95 % confidence interval for the calibration (dashed lines); the equation for the calculated calibration curve is y = 3431 + 146 x, where y is Raman intensity and x is bilirubin concentration (nM).

The calibration curve for bilirubin quantification with SERRS is presented in Figure 13, using the intensity of the bilirubin band at 680 cm^{-1}. The lowest concentration measured was 10 nM, which is three orders of magnitude lower than the lowest concentration previously reported, as detected with SERRS [8,10]. For concentrations between 10 nM and 200 nM the correlation between the spectrum intensity and the bilirubin concentration is linear (Figure 13b), with a coefficient of determination (R^2) of 0.9979. For concentrations lower than 10 nM the spectrum does not show bilirubin vibrational bands. On the contrary, for concentrations higher than 200 nM the signal doesn't increase, likely because the surface of the PLL-AgNPs is

saturated by bilirubin molecules. The limit of detection (LOD) and the limit of quantification (LOQ) calculated from the calibration curve are 24 nM and 45 nM, respectively. The LOD is the lowest quantity of analyte that can be distinguished from the a blank value within a stated confidence limit and the LOQ is the lowest amount of analyte in a sample that can be quantitatively determined with suitable precision and accuracy.

3.4 Conclusions

The preparation of PLL-coated silver nanoparticles was reported, and consistent results from UV-vis, TEM, z-potential, DLS and SERS microscopy prove that the PLL forms a positively-charged polymer layer around the nanoparticles, without inducing their aggregation. This study demonstrates that the PLL coated nanoparticles can be used as stable, reproducible and efficient SERS substrates for detection and quantification of anionic chromophores such as bilirubin. Because of its characteristics, such substrate could be also applied for the SERRS based quantification of other negatively charged analytes, such as dye-labeled DNA [29].

3.5 References

[1] H Munro, W E Smith, M Garner, J Clarkson, and P C White, "H. Munro, W. E. Smith,Characterization of the Surface of a Citrate-Reduced Colloid Optimized for Use as a Substrate for Surface-Enhanced Resonance Raman Scatterin," *Langmuir*, vol. 11, pp. 3712-3720, 1995.

[2] J D Ostrow, P Mukerjee, and Claudio Tiribelli, "Structure and binding of unconjugated bilirubin: Relevance for physiological and pathophysiological

function," *Journal of lipid research*, vol. 35, pp. 1715-1737, 1994.

[3] Y Z Hsieh and M D Morris, "Resonance Raman spectroscopic study of bilirubin hydrogen bonding in solutions and in the albumin complex," *Journal of the American Chemical Society*, vol. 110, pp. 62-67, 1988.

[4] L Margulies and M Toporowicz, "Resonance raman and electronic absorption spectroscopy of bilirubin in solution. An experimental and theoretical study," *Journal of Molecular Structure*, vol. 174, pp. 153-158, 1988.

[5] B Yang, M D Morris, M Xie, and D A Lightner, "Resonance Raman spectroscopy of bilirubins: Band assignments and application to bilirubin/lipid complexation," *Biochemistry*, vol. 30, pp. 688-694, 1991.

[6] E Hu, F Liang, Duschek, and W Kiefer, "Resonance Raman spectroscopic study of free brilirubin and brilirubin complexes with copper(II), silver(I) and gold(III)," *Spectrochimica Acta Part A: Molecular and Biomolecular Spectroscopy*, vol. 53, pp. 1431-1438., 1997.

[7] J Yin and H Watarai, "Resonance raman spectroscopic study on chiral aggregation of bilirubin-bovine serum albumin complex formed at liquid/liquid interface," *Analytical sciences: the international journal of the Japan Society for Analytical Chemistry*, vol. 23, pp. 841-846, 2007.

[8] Y Z Hsieh, N S Lee, R S Sheng, and M D Morris, "Surface-enhanced Raman spectroscopy of free and complexed bilirubin," *Langmuir*, vol. 3, pp. 1141-1146, 1987.

[9] J Chen, J Hu, Z Xu, and R S Sheng, "Surface-enhanced Raman spectroscopy of free bilirubin and bilirubin complexes with transition metals iron(II), nickel(II) and cobalt(II)," *Spectrochimica Acta Part A: Molecular Spectroscopy*, vol. 50, pp. 929-

936, 1994.

[10] R Sulk et al., "Surface-enhanced Raman assays (SERA): Measurement of bilirubin and salicylate," *Journal of Raman Spectroscopy*, vol. 30, pp. 853-859, 1999.

[11] P C Lee and D Meisel, "Adsorption and surface-enhanced Raman of dyes on silver and gold sols Adsorption and Surface-Enhanced Raman of Dyes on Silver and Gold Sols," *J. of Phys. Chem.*, vol. 86, pp. 3391-3395, 1982.

[12] M Potara, D Maniu, and S Astilean, "The synthesis of biocompatible and SERS-active gold nanoparticles using chitosan," *Nanotechnology*, vol. 20, p. 315602, 2009.

[13] S Sanchez-Cortes and J V Garcia-Ramos, "Anomalous Raman bands appearing in surface-enhanced Raman spectra," *J.Raman Spectrosc*, vol. 29, p. 365–371, 1998.

[14] R Development Core Team, R: A language and environment for statistical computing., 2010.

[15] L Gong, W Constantine, and Y A Chen, msProcess: Protein Mass Spectra Processing, 2009.

[16] C Beleites and Valter Sergo, hyperSpec: a package to handle hyperspectral data sets in R, in preparation for Journal of Statistical Software, R package version 0.95.

[17] J Ranke, chemCal: Calibration functions for analytical chemistry, 2007.

[18] G. Smith and E Dent, *Modern Raman spectroscopy: a practical approach.* Chichester, U.K.: John Wiley and Sons, 2005.

[19] R. Aroca, *Surface enhanced vibrational spectroscopy.* Chichester, U.K.: John Wiley and Sons, 2006.

[20] T M Riddick, *Control of stability Through Zeta Potential*. New York: Zeta Meter Inc,

1968.

[21] R A Alvarez-Puebla and R F Aroca, "Synthesis of Silver Nanoparticles with Controllable Surface Charge and Their Application to Surface-Enhanced Raman Scattering," *Anal.Chem*, vol. 81, pp. 2280-2285, 2009.

[22] S Tan, M Erol, A Attygalle, H Du, and S A Sukhishvili, "Synthesis of Positively Charged Silver Nanoparticles via Photoreduction of AgNO3 in Branched Polyethyleneimine/HEPES Solutions," *Langmuir*, vol. 23, pp. 9836-9843, 2007.

[23] J A Creighton, *Spectroscopy of Surfaces*. Chichester: Wiley, Chichester, 1988.

[24] D Carrier and M Pezolet, "Raman spectroscopic study of the interaction of poly-L-lysine with dipalmitoylphosphatidylglycerol bilayers," *Biophys.J*, vol. 46, pp. 497-506, 1984.

[25] L Guerrini et al., "Importance of metal-adsorbate interactions for the surface-enhanced Raman scattering of molecules adsorbed on plasmonic nanoparticles," *Plasmonics*, vol. 2, p. 147−156, 2007.

[26] T M Herne and R L Garrell, "Borate interference in surface-enhanced Raman spectroscopy of amines.," *Anal.Chem.*, vol. 63, p. 2290−2294, 1991.

[27] W E Smith and C Rodger, *Handbook of Vibrational Spectroscopy*. Chichester, U.K.: John Wiley & Sons, 2002.

[28] P A Zunszain, J Ghuman, A F McDonagh, and S Curry, "Crystallographic analysis of human serum albumin complexed with 4Z,15E-Bilirubin-Ixα.," *J.Mol.Biol.*, vol. 394-406, p. 381, 2008.

[29] D Graham and K Faulds, "Quantitative SERRS for DNA sequence analysis," *Chem. Soc. Rev.*, vol. 37, pp. 1042-1051, 2008.

Chapter 4:

SERRS substrate suitable for measuring bilirubin cellular up-take

4.1 Introduction

Bilirubin is generally regarded as cytotoxic, as said in chapter 2. However recent studies have demonstrated that low concentration of bilirubin exhibits anti-oxidant properties [1-3]. Hence, there is an increasing interest in the bilirubin up-take mechanism and quantification [4, 5]. Since the cellular medium contained bilirubin at nanomolar concentration [4] the poly-L-lysine coated nanoparticles (PLL-AgNPs), described in chapter 3, could be applied to quantify the amount of bilirubin that remains in the cellular medium. In this way the bilirubin up-take of cell cultures could be measured indirectly.

Since the buffer used to prepare bilirubin solution in the experiments described in chapter 3 (old buffer), is not suitable for cell growth, a new one was developed. This new buffer have the same ionic strength of the old buffer, to be suitable for SE(R)RS measurement, but the osmolarity and a lower pH (pH 7.4) were chosen considering the cell growth.

In this chapter, the applicability of PLL-AgNPs to measure the bilirubin in this new buffer was evaluated. However, the bilirubin spectrum intensity with this new buffer is lower than the spectrum intensity with the old buffer reported in chapter 3. A possible reason could be the different protonation state of the poly-L-Lysine (PLL) at a lower pH.

To substitute the PLL two positively charged polymers that contain a quaternary nitrogen atom (poly-N^+) were chosen. Poly-N^+ compounds belongs to a class of polyelectrolytes that derive unique properties mainly from the density and distribution of positive charges along the macromolecular structure[6].

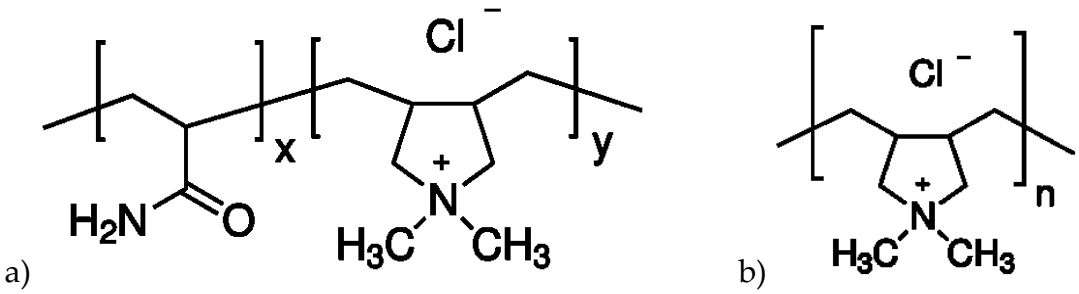

Figure 14: General structure of the poly-N^+ used to coat the AgNPs: a) (P(AAm-DADMAC), b) P(DADMAC).

One of the poly-N^+ is a copolymer with an acrylamide part and a diallyldimethylammonium part (P(AAm-DADMAC)), the second one has just the diallyldimethylammonium part (P(DADMAC)). The poly-N^+ general structure is reported in Figure 14. Thanks to the presence of the quaternary nitrogen atom, the charge of this polymer do not depend on pH.

In this chapter the development of a SE(R)RS-substrate consisting of citrate reduced silver nanoparticles coated with poly-N^+ (poly-N^+-AgNPs) and their characterization using UV-Vis spectrophotometry was reported.

The Lee-Meisel procedure [7] was choosen to synthesized silver nanoparticles, since its enhancement properties with bilirubin was already investigated in the chapter 3. The ability of the poly-N^+-AgNPs to detect bilirubin was evaluated.

4.2 Experimental section

4.2.1 Materials

Silver Nitrate (AgNO3), dimethyl sulfoxide (DMSO), sodium citrate tribasic dehydrate, poly-L-lysine hydro-bromide (PLL) (mol wt 15,000-30,000), poly(acrylamide-co-diallyldimethylammonium chloride) solution 10% in water (P(AAm-DADMAC)), poly(diallyldimethylammonium chloride) (average Mw <100,000) solution 35 wt. % in water (P(DADMAC)), bilirubin (mixture of isomers (IIIA, VIIIA and IXA)), K_2HPO_4 and KH_2PO_4, sucrose, sodium chloride and sodium hydroxide were purchased from Sigma-Aldrich. All chemicals were used without further purification.

Ultra pure Milli-Q water (Merck Millipore, Billerica, MA, USA) was used for the preparation of all solutions.

4.2.2 Nanoparticles synthesis and Poly-L-lysine coated silver nanoparticles (PLL-AgNPs) preparation

The Cit-AgNPs and PLL-AgNPs were prepared according to the procedure described in chapter 3. The Cit-AgNPs were prepared according to the procedure described by Lee and Meisel [7]. The $AgNO_3$ solution was heated to boiling point under reflux and the tri-sodium citrate aqueous solution (1% w/v) was added. The mixture was kept boiling under reflux and stirring for 1 h and then slowly cooled

down to room temperature. The PLL-AgNPs were prepared adding 0.1% w/v poly-L-lysine aqueous solution was prepared to the Cit-AgNPs. The mixture was centrifuged at 6708 × g for 20 minutes, the supernatant was removed and fresh Milli-Q water was added. This washing procedure was repeated 3 times. Before its use as SERS substrate, the stock dispersion of coated nanoparticles was pelleted by centrifugation.

4.2.3 *Nanoparticles coated with Poly-N^+ preparation*

A 0.1% w/v P(AAm-DADMAC) aqueous solution and a 10% w/v P(DADMAC) was prepared. Two batches NPs were coated: under vigorous stirring, in the first case 50 mL of the P(AAm-DADMAC) solution, in the second case 50 mL of the P(DADMAC) were added to 50 mL of Cit-AgNPs previously diluted 1:10 with Milli-Q water. In order to remove the polymer excess, the two mixtures were centrifuged in 1.5 mL polypropylene eppendorf tubes at 6708 × g for 20 minutes, the supernatant was removed, fresh Milli-Q water was added and the redispersed NPs were sonicated for 30 min. This washing procedure was repeated 3 times.

The resulting coated-nanoparticles dispersion is stable against aggregation for some days. Before their use as SERRS substrate, the two stock dispersions of coated nanoparticles were pelleted by centrifugation and removal from each eppendorf tube of 1.3 mL of the supernatant with a micropipette, resulting in a concentrated aqueous dispersion of coated nanoparticles.

4.2.4 *Buffer preparation*

Old phosphate buffer solution 20 mM with pH 8.00 (ionic strength = 0.055 mol·dm^3 and osmolarity = 0.057 osmol/L), used also for the experiment reported in chapter 2.2, was prepared using K_2HPO_4 and KH_2PO_4.

The new buffer at pH 7 (ionic strength = 0.055 mol·dm^{-3} and osmolarity = 0.263 osmol/L), was prepared dissolving in 50 mL of Milli-Q water 49.7 mg of K_2HPO_4, 109.7 mg of KH_2PO_4, 3.29 g of sucrose and 27.8 mg of NaCl.

4.2.5 *Bilirubin solutions*

A bilirubin stock solution was prepared dissolving bilirubin in anhydrous dimethyl sulfoxide to obtain a final concentration of 5 mM. 100 μM bilirubin solutions were prepared diluting 50 times the stock solution with a 10 mM NaOH aqueous solution. Two batches of 100 nM bilirubin solution was prepared: one using the old buffer (pH 8), one using the new buffer (pH 7.4) for dilution. Extreme care was taken to avoid bilirubin photodegradation upon light exposure: all dilutions were done in a dark room with red safelight illumination.

4.2.6 *Raman instrumentation*

Spectroscopic measurements were done using an inVia Raman system (Renishaw, Wotton-under-Edge, UK). As laser sources a 514.5 nm argon-ion laser was focused on the samples through a 10× objective (0.25 N.A.). The 514.5 nm laser power at the sample was 650 μW to avoid bilirubin photodegradation. SERRS spectra of bilirubin were collected with an acquisition time of 50 s. To 2.5 μL of the PLL-AgNPs were added 50 μL of bilirubin solution (old buffer with pH 8 or new buffer with pH 7.4). To 10 μL of the poly-N^+-NPs were added 30 μL of bilirubin solution (old buffer pH 8). Extreme care was taken to avoid bilirubin photodegradation upon laser exposure.

4.2.7 *Nanoparticles characterization:*

UV-Vis spectra were acquired with a Perkin Elmer Lambda bio20 spectrophotometer, between 350 nm and 700 nm. Samples were prepared by diluting 10× the silver nanoparticles stock solution with Milli-Q water in a 3 mL cuvette.

4.2.8 *Data processing*

All data pre-processing and analysis was performed using several packages of the R software for statistical analysis [9]. The position of the bands was estimated with msProcess [10], a package providing tools for spectra processing. SERRS spectra were analyzed with hyperSpec [11], an R package to handle hyperspectral data sets, in this case spectra plus concentrations.

4.3 Results and discussion

The PLL-AgNPs characterization and their application to quantify bilirubin were reported in details in chapter 3. Briefly those nanoparticles have an absorption maximum at 410 nm and the ζ-potentials +62.3 ± 1.6 mV.

Figure 15 show the SERRS spectrum of 100 nM bilirubin solution, prepared using the new buffer (pH 7.4) with PLL-AgNPs. The spectrum presents vibrational bands at 1617 cm^{-1}, 1580 cm^{-1}, 1460 cm^{-1}, 1340 cm^{-1}, 1271 cm^{-1}, 1190 cm^{-1}, 990 cm^{-1}, 960 and at 690 cm^{-1}, in accordance with bilirubin resonance Raman spectra described in literature [12][13][14], and with bilirubin SERRS spectrum reported in chapter 2.2. A possible band assignment is also presented in chapter 3.

As shown in Figure 16, the bilirubin SERRS spectrum intensity is lower with the new buffer than with the old buffer. Reasonably the PLL have a different protonation

state at a lower pH. Hence, the affinity between bilirubin and the PLL-AgNPs is reduce, because the electrostatic forces operating between opposite charges are lower.

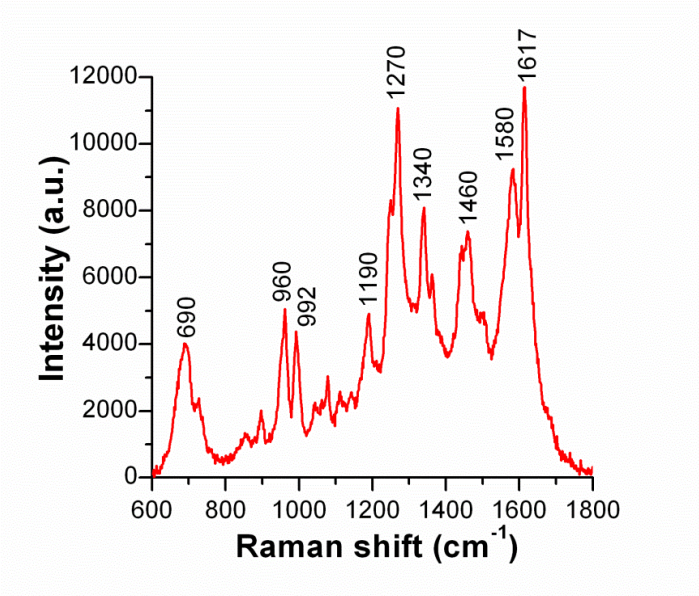

Figure 15: Bilirubin SERRS spectrum with PLL-AgNPs using the new buffer (pH = 7,4).

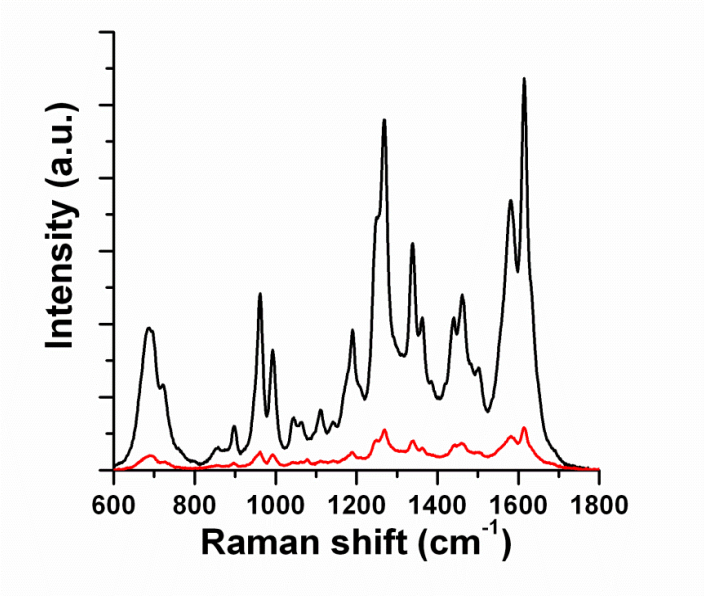

Figure 16: Comparison between SERRS spectrum of 100 nM bilirubin solution prepared using the new buffer (red line); and SERRS spectrum of 100 nM bilirubin solution prepared using the old buffer (black line).

As said in chapter 3, a high affinity of the analyte for the metal substrate is an essential requirement for obtaining a SERS signal.

The bilirubin SERRS intensities at 690 cm^{-1} as a function of bilirubin concentration measured in the experiment with the PLL-AgNPs and the new buffer is reported in Figure 17. As shown in the picture, the intensity do not vary appreciably as a function of bilirubin concentration and the 200 nM intensity value presents a large dispersion. For this reason the calculation of a calibration curve with the purpose of bilirubin quantification in sample with unknown concentration was not possible.

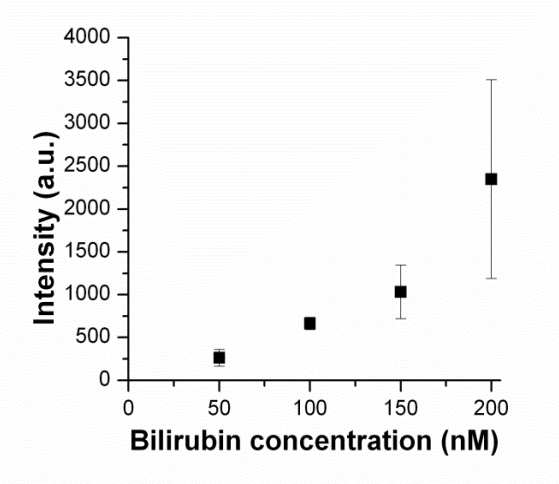

Figure 17: Bilirubin SERRS intensities at 690 cm^{-1} as a function of bilirubin concentration: intensity average value of the band at 690 cm^{-1} (black square) with standard deviations.

4.3.1 Poly-N^+ coated nanoparticles characterization

The Cit-AgNPs have an absorption maximum at 405 nm (Figure 18, black line), as reported in literature [7] and chapter 3.

The P(AAm-DADMAC)-AgNPs have an absorption maximum at 410 nm (Figure 18A, blue line). This red shift of the plasmonic frequency from 405 to 410 nm can be attributed to the adsorption of the P(AAm-DADMAC) on the nanoparticles

surface, indicating that the coating succeeded. The relatively small 5 nm red shift rules out the formation of large nanoparticles aggregates upon P(AAm-DADMAC) coating.

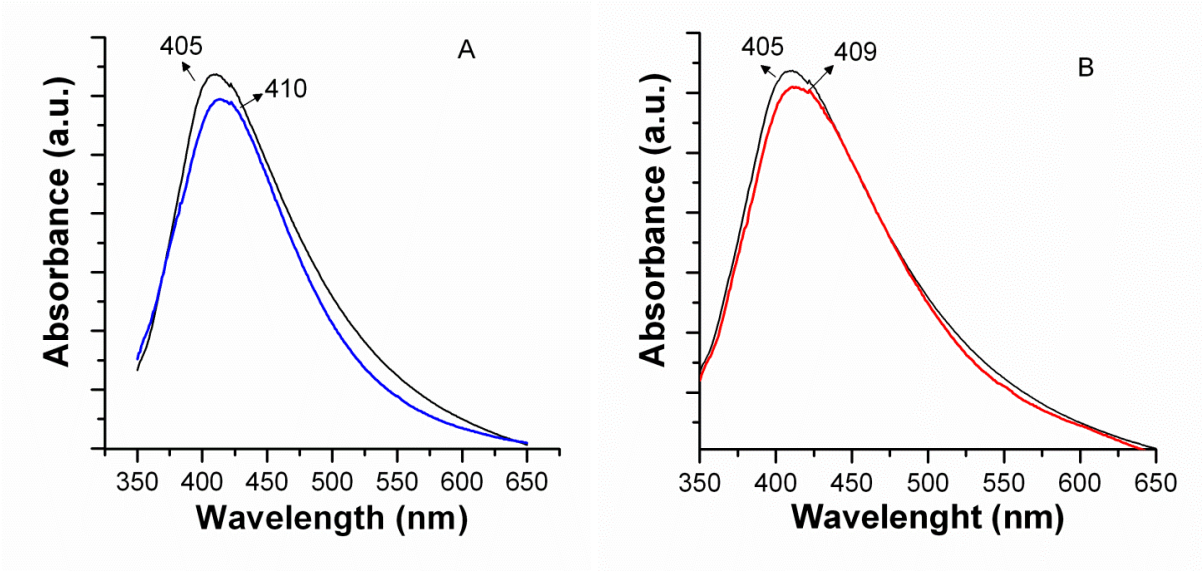

Figure 18: UV-vis extinction spectra of Cit-AgNPs (black line), P(AAm-DADMAC)-AgNPs (A, blue line) and b) P(DADMAC)-AgNPs (B, red line)

The P(DADMAC)-AgNPs show an absorption maximum at 409 nm (Figure 18B, red line). As said for the P(AAm-DADMAC)-AgNPs, this small red shift, from 405 to 409 nm, suggests that the P(DADMAC) is adsorbed on the nanoparticles surface and no aggregation occurs during the coating process.

4.3.2 Interaction of the bilirubin with poly-N⁺

The bilirubin SERRS spectrum using the Cit-AgNPs as substrate did not show any vibrational bands (Figure 18 and Figure 20, black line), as reported in chapter 3.

The bilirubin SERRS spectra in the presence of the P(AAm-DADMAC)-AgNPs (Figure 19, blue line) shows vibrational bands at 1617 cm^{-1}, 1580 cm^{-1}, 1450 cm^{-1}, 1335

cm^{-1}, 1266 cm^{-1}, 1190 cm^{-1}, 996 cm^{-1}, 960 and at 692 cm^{-1}. Likewise bilirubin SERRS spectra in the presence of the P(DADMAC)-AgNPs (Figure 20 red line) shows vibrational bands at 1614 cm^{-1}, 581 cm^{-1}, 1456 cm^{-1}, 1334 cm^{-1}, 1261 cm^{-1}, 1191 cm^{-1}, 990 cm^{-1}, 961 and at 682 cm^{-1}.

This vibrational features are in accordance with previous studies on the RR spectrum of bilirubin [12][13][14], and the results for SERRS measurement reported in chapter 3, where a detail band assignment was also reported. The presence of those band demonstrated that the bilirubin is able to interact with the two poly-N^+, P(AAm-DADMAC) and P(DADMAC), chosen to substitute the PLL.

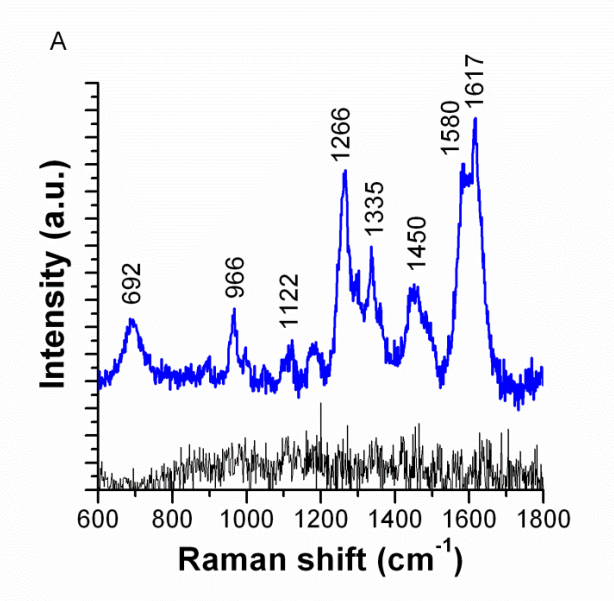

Figure 19: Comparison of resonance Raman spectrum of 100 nM bilirubin (black line) and SERRS spectrum of 100 nM bilirubin in the presence of P(AAm-DADMAC)-AgNPs (blue line); B)

This results shown that is possible to detect nanomolar concentration of bilirubin. The concentration measured was 100 nM, which is two orders of magnitude lower than the lowest concentration previously reported in literature [15], [16].

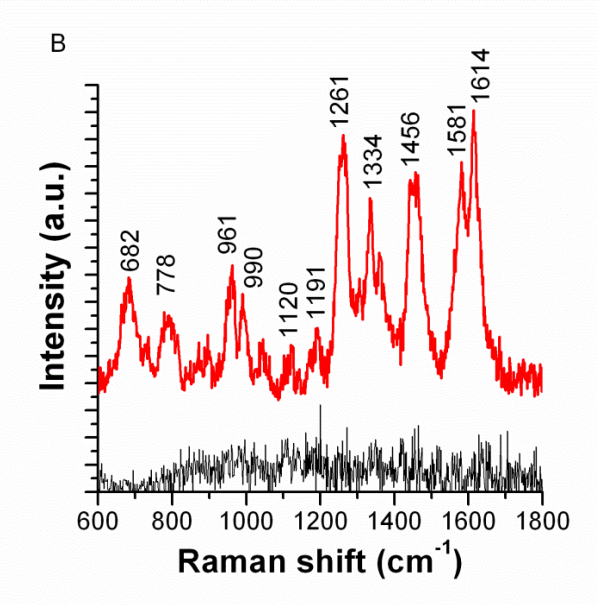

Figure 20: Comparison of resonance Raman spectrum of 100 nM bilirubin (black line) and SERRS spectrum of 100 nM bilirubin in the presence of P(DADMAC)-AgNPs (red line).

To improve the efficiency and reproducibility of the SERRS substrates some preliminary experiment were performed, demonstrating that is possible immobilize the Cit-AgNPs on a glass slide using the two poly-N^+, as represented in the scheme in Figure 21.

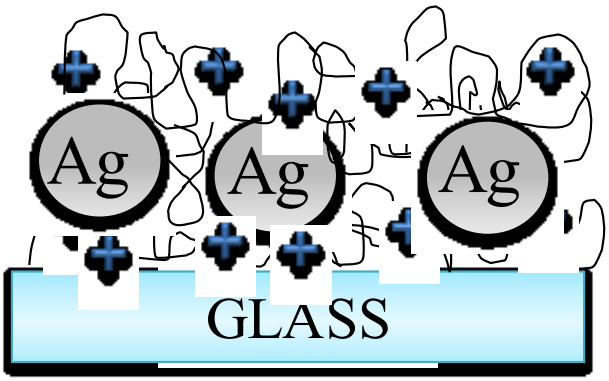

Figure 21: Scheme of the Cit-AgNPs immobilize on a glass slide using the poly-N^+.

4.4 Conclusion

The application of PLL-AgNPs to measure indirectly the bilirubin cellular uptake was proposed. A new buffer, with the same ionic strength of the one described in chapter 3, and the osmolarity and pH suitable for cell growth was developed. The ability of the PLL-AgNPs to detect the bilirubin in the new buffer solution was verified, but the bilirubin quantification is not possible. A new substrate was developed to overcome this problem. The Cit-AgNPs were coated with P(AAm-DADMAC) and P(DADMAC). The possibility to detect 100 nM bilirubin concentration with those substrates was demonstrated.

Some preliminary experiment demonstrated that the Cit-AgNPS can be immobilize on a glass slide using the P(AAm-DADMAC) and P(DADMAC). Those promising substrate should be characterized and optimized for measuring bilirubin.

4.5 References

[1] M. S. Shahab, P. Kumar, N. Sharma, A. Narang e R. Prasad, «Evaluation of oxidant and antioxidant status in term neonates:a plausible protective role of bilirubin,» *Mol Cell Biochem,* vol. 317, pp. 51 - 59, 2008.

[2] M. L. Tomaro e A. M. del C. Batle, «Bilirubin: its role in cytoprotection against oxidative stress,» *The International Journal of Biochemistry & Cell Biology,* vol. 34, pp. 216 - 220, 2002.

[3] L. Žiberna, G. Drevenšek, F. Tramer e S. Passamonti, «Cellular antioxidant activity of bilirubin in the human endothelial cell line EA.hy 926 is mediated by

bilitranslocase,» *BMC Pharmacology,* vol. 9 (Suppl 2) : A57, 2009.

[4] S. Passamonti, M. Terdoslavich, A. Margon, A. Cocolo, N. Medic, F. Micali, G. Decorti e M. Frank, «Uptake of bilirubin into HepG2 cells assayed by thermal lens spectroscopy - Function of bilitranslocase,» *FEBS Journal,* vol. 272, p. 5522 – 5535, 2005.

[5] A. Margon, M. Terdoslavich, A. Cocolo, G. Decorti, S. Passamonti e M. Franko, «Determination of bilirubin by thermal lens spectrometry and studies of its transport into hepatic cells,» *Journal De Physique. IV : JPVolume 125, 2005, Pages 717-720,* vol. 125, pp. 717 - 720, 2005.

[6] W. Jaeger, J. Bohrisch e A. Laschewsky, «Synthetic polymers with quaternary nitrogen atoms—Synthesis and structure of the most used type of cationic polyelectrolytes,» *Progress in Polymer Science,* vol. 35, pp. 511 - 577, 2010.

[7] P. C. Lee e D. Meisel, «Adsorption and surface-enhanced Raman of dyes on silver and gold sols Adsorption and Surface-Enhanced Raman of Dyes on Silver and Gold Sols,» *J. of Phys. Chem.,* vol. 86, pp. 3391-3395, 1982.

[8] M. Potara, D. Maniu e S. Astilean, «The synthesis of biocompatible and SERS-active gold nanoparticles using chitosan,» *Nanotechnology,* vol. 20, p. 315602, 2009.

[9] R Development Core Team, *R: A language and environment for statistical computing.,* Vienna, Austria: R Foundation for Statistical Computing, url http://www.R-project.org, 2010.

[10] L. Gong, W. Constantine e Y. A. Chen, *msProcess: Protein Mass Spectra Processing,* 2009.

[11] C. Beleites e V. Sergo, *hyperSpec: a package to handle hyperspectral data sets in R, in preparation for Journal of Statistical Software, R package version 0.95.*

[12] B. Yang, M. D. Morris, M. Xie e D. A. Lightner, «Resonance Raman spectroscopy of bilirubins: Band assignments and application to bilirubin/lipid complexation,» *Biochemistry,* vol. 30, pp. 688-694, 1991.

[13] J. Yin e H. Watarai, «Resonance raman spectroscopic study on chiral aggregation of bilirubin-bovine serum albumin complex formed at liquid/liquid interface,» *Analytical sciences: the international journal of the Japan Society for Analytical Chemistry,* vol. 23, pp. 841-846, 2007.

[14] J. Hu, T. Wang, D. Moigno, M. Wumaier, W. Kiefer, J. Mao, Q. Wu, F. Niu, Y. Gu, Q. Chen, J. Ma e H. Feng, «Fourier-transform Raman and infrared spectroscopic analysis of dipyrrinones and mesobilirubins.,» *Spectrochim. Acta, Part A,* vol. 57, p. 2737–2743, 2001.

[15] Y. Z. Hsieh, N. S. Lee, R. S. Sheng e M. D. Morris, «Surface-enhanced Raman spectroscopy of free and complexed bilirubin,» *Langmuir,,* vol. 3, pp. 1141-1146, 1987.

[16] R. Sulk, C. Chan, J. Guicheteau, C. Gomez, J. B. B. Heyns, R. Corcoran e K. Carron, «Surface-enhanced Raman assays (SERA): Measurement of bilirubin and salicylate,» *Journal of Raman Spectroscopy,* vol. 30, pp. 853-859, 1999.

Chapter 5:

Development of SERRS substrates for measuring bilirubin in the presence of albumin

5.1 Introduction

As mentioned in chapter 2, the bilirubin in the serum is present in three form: as free bilirubin, bilirubin bonded with albumin and sugar-conjugated bilirubin [1].

In this chapter the application of the poly-L-lysine coated nanoparticles (PLL-AgNPs), described in chapter 3, to quantify bilirubin in the presence of human serum albumin (HSA) will be described. The effect of HSA on the bilirubin SERRS intensity was investigated. The interaction between the PLL-AgNPs and HSA was studied using TEM, showing the HSA bonded with the PLL layer around NPs. Hence the bilirubin cannot interact with the nanoparticles because of a layer of HSA around the NPs.

Since bilirubin is considered itself hydrophobic [1], due to the presence of many hydrophobic groups [2], to overcome the problem of the HSA layer around the

nanoparticles an hydrophobic capping and the transfer of the NPs to an organic phase was considered.

The nanoparticles phase transfer from aqueous solution to organic phase can be achieved after a capping exchange using alkylamines. The capping exchange is based on electrostatic interaction between negatively charged surface groups of the metal nanoparticles (COO^-) and the positively charged NH_3^+ groups of alkylamines, such as octadecylamine (ODA) [3]. Different procedures for the phase transfer for small (diameter < 20 nm) gold nanoparticles are reported in literature [4,5], where the NPs capping exchange and the NPs move in the final organic phase at the same time. But those procedures does not work for NPs with larger size. Wang and colleagues [6] used ODA dissolved in ethanol as capping agent to extract the metal NPs from the colloidal suspension.

In this work a modified version of this procedure was applied to extracts the Cit-AgNPs from the aqueous suspension. After drying the ODA-Cit-AgNPs were re-dispersed in hexane.

To improve the reproducibity of the silver nanoparticles synthesis the protocol described by Leopold and Lendl [7] was considered. Some preliminary experiment for the phase transfer of the LL-AgNPs were performed.

5.2 Experimental section

5.2.1 Materials:

Silver Nitrate ($AgNO_3$), sodium citrate tribasic dehydrate, hydroxylamine hydrochloride, sodium hydroxide, dimethyl sulfoxide (DMSO), poly-L-lysine hydro-bromide (PLL) (mol wt 15,000-30,000), human serum albumin (HSA), octadecylamine

and ethanol were purchased from Sigma-Aldrich. All chemicals were used without further purification. Ultra pure Milli-Q water (Merck Millipore, Billerica, MA, USA) was used for the preparation of all solutions.

5.2.2 *Nanoparticles synthesis:*

Cit-AgNPs were prepared according to the procedure described by Lee and Meisel [8], and in chapter 3.

The LL-AgNPs were synthesized following the procedure described by Leopold and Lendl [7]. Briefly, 10,44 mg of hydroxylamine HCl were dissolved in 90 mL of 3.33 10^{-3} M sodium hydroxide solution. At room temperature and stirring constantly, 10 mL of 10^{-2} M of $AgNO_3$ were added dropwise to the hydroxylamine solution.

All glassware was thoroughly cleaned using concentrated HNO_3 and then chromic acid (2.77 g $K_2Cr_2O_7$ in 100 mL H_2SO_4), and carefully rinsed with Milli-Q water.

5.2.3 *Poly-L-lysine coated silver nanoparticles (PLL-AgNPs) preparation*

The PLL-AgNPs were prepared according to the procedure described in chapter 3. Briefly, the PLL-AgNPs were prepared adding 0.1% w/v poly-L-lysine aqueous solution was prepared to the Cit-AgNPs. The mixture was centrifuged at 6708 ⊙ g for 20 minutes, the supernatant was removed and fresh Milli-Q water was added. This washing procedure was repeated 3 times. Before its use as SERS substrate, the stock dispersion of coated nanoparticles was pelleted by centrifugation.

5.2.4 Nanoparticles phase transfer:

To transfer the Ag nanoparticles from aqueous to organic phase the procedure proposed by Wang [6] was modified as follow. The same volume of 10 nM ODA ethanol solution was added to the AgNPs suspension in a glass tube suitable for centrifuging. The mixture was vigorously shacked using a magnetic stir bar for 10 s. All the water was removed by centrifugation and 48 h of drying in oven and the ODA-NPs were redispersed into hexane. The so-obtain suspension was sonicated, centrifuged and fresh hexane was added to remove the excess of ODA. This washing procedure was repeated two times. The ODA-Cit-AgNPs are stable in hexane for weeks.

The same procedure was used to transfer the LL-AgNPs from aqueous to organic phase.

5.2.5 Bilirubin and HSA solutions

A bilirubin stock solution was prepared dissolving bilirubin in anhydrous dimethyl sulfoxide to obtain a final concentration of 5 mM. 100 μM bilirubin solutions were prepared diluting 50 times the stock solution with a 10 mM NaOH aqueous solution. The 800 nM bilirubin solution were prepared using a 20 mM buffer phosphate solution (pH 8), to obtain obtaining a final bilirubin concentration of 400 nM after adding the HSA.

The HSA solution was prepared using the same 20 mM buffer phosphate solution (pH 8). The bilirubin-HSA solution was prepared immediately before measuring the SERRS spectrum. The same volume of HSA was added to the same volume of 800 nM bilirubin solution.

Extreme care was taken to avoid bilirubin photodegradation upon light exposure: all dilutions were done in a dark room with red safelight illumination.

5.2.6 Instrumentation

Spectroscopic measurements were done using an inVia Raman system (Renishaw, Wotton-under-Edge, UK). As laser sources a 514.5 nm argon-ion laser was focused on the samples through a 10× objective (0.25 N.A.). The 514.5 nm laser power at the sample was 650 μW to avoid bilirubin photodegradation. SERRS spectra of bilirubin were collected with an acquisition time of 50 s. To 2.5 μL of the PLL-AgNPs were added 50 μL of bilirubin or bilirubin-HSA solution. Extreme care was taken to avoid bilirubin photodegradation upon laser exposure.

Transmission electron microscopy (TEM) was performed with a Philips EM208 scanning electron microscope using a carbon coated nickel grid (Carbon Film 200 Mesh, Ni, 50/bx produced by Electron Microscopy Sciences). Uranyl acetate ($UO_2(CH_3COO)_2 \bullet 2H_2O$) was added to samples composed of PLL-AgNPs and HSA on the TEM grids as contrast agent, to visualize the positively charged organic layer around the NPs and the human serum albumin, as reported in literature for the chitosan [9].

5.2.7 Data processing

As reported in chapter 3, all data pre-processing and analysis was performed using several packages of the R software for statistical analysis [9]. The position of the bands was estimated with msProcess [10], a package providing tools for spectra processing. SERRS spectra were analyzed with hyperSpec [11], an R package to handle hyperspectral data sets, in this case spectra plus concentrations.

5.3 Results and discussion

5.3.1 Interaction between HSA and PLL-AgNPs

In Figure 22 is reported the SERRS intensities at 690 cm^{-1} of 400 nM free bilirubin solution as a function of the HSA concentration added to the 400 nM bilirubin solution. As expected, increasing the amount of HSA the bilirubin signal decreases. As a result of the large number of potentially reactive groups, the free bilirubin rapidly associate with albumin, through a network of reversible hydrogen bonds [13]. Hence, most reasonably, the amount of free bilirubin that can interact with the PLL-AgNPs decrease after adding HSA because the albumin bound the free bilirubin

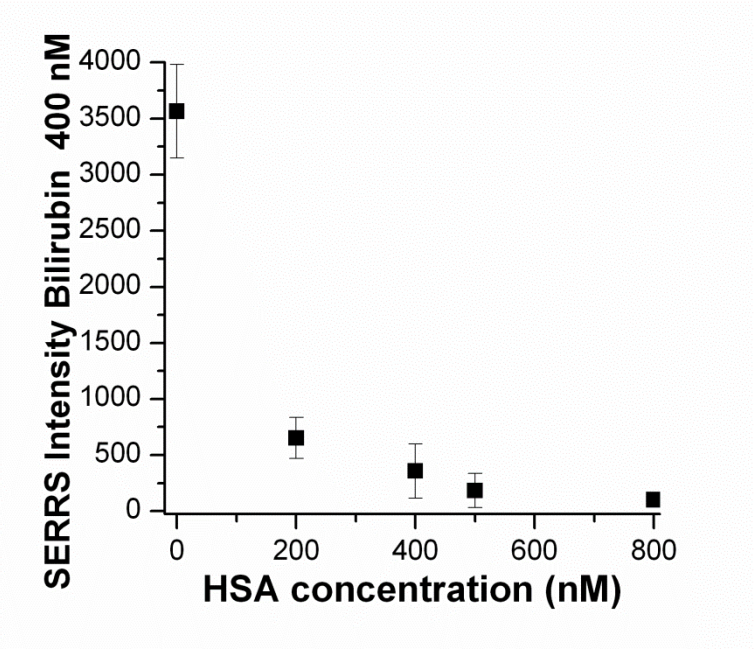

Figure 22: SERRS intensities at 690 cm^{-1} of bilirubin 400 nM as a function of HSA concentration.

The HSA was added to the PLL-AgNPs and the TEM images show a second layer around the metal nanoparticles (Figure 23). The first layer was already indentify

as PLL in chapter 3. The second layer could be the HSA bonded on the PLL layer around NPs. The affinity between PLL and bovine serum albumin (BSA) was shown in literature [14] [15], since the positively charged functional group of PLL could combine with the negatively charged HSA. Furthermore, the formation a protein-coronas around nanoparticles under physiological condition, changing the surface functionality of NPs, was recently reported in literature [16], [17], [18]. The formation of the corona is essentially a competition of proteins and other bio-molecules for binding to the NP surface [19]. Hence bilirubin cannot interact with the nanoparticles surface and the bilirubin 400 nM SERRS intensity decreases (Figure 22).

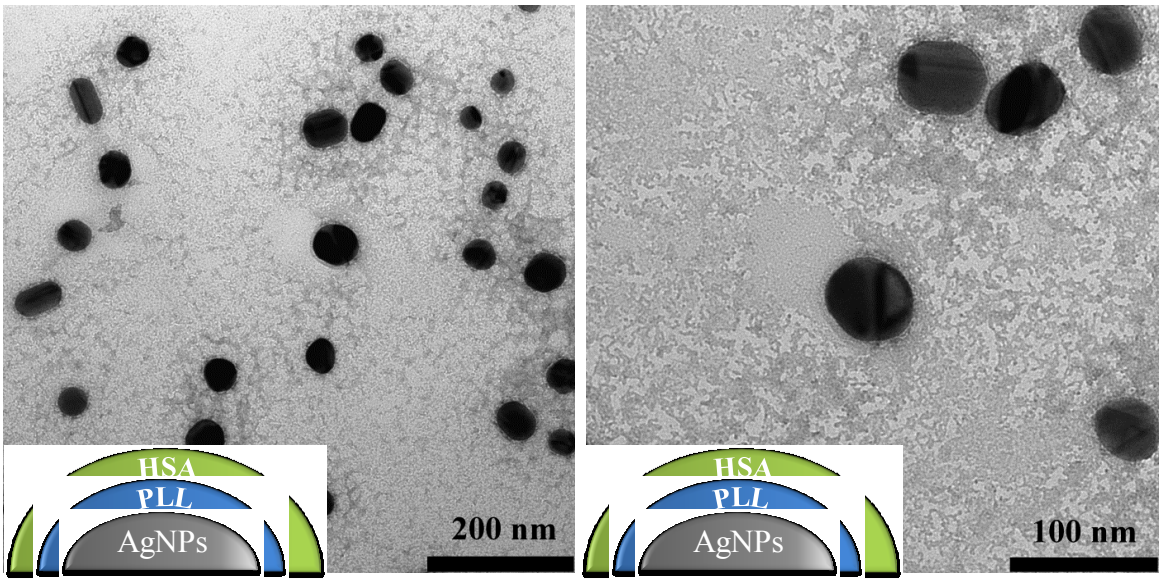

Figure 23: TEM images of Pll-AgNPs with HSA treated with uranyl acetate ($UO_2(CH_3COO)_2 \cdot 2H_2O$) to enhance the contrast due to the HSA and PLL layer around the silver nanoparticles.

5.3.2 Silver nanoparticles with hydrophobic capping

The 10 nM ODA ethanol solution was added to the AgNPs suspension and the two phase remain separated, in particular the nanoparticles remains in the bottom part of the flask and the ODA ethanol solution in the upper part (Figure 24A). After a

vigorous shacking (Figure 24B), the mixture spontaneously separated in two phase (Figure 24C). In particular the AgNPs moves to the upper phase, indicating that the capping exchange succeeded. To re-disperse the so-obtained ODA-LM-AgNPs into hexane is strictly necessary to remove all the water with centrifugation and a drying. After the dispersion in hexane, the excess of ODA must be removed through a washing procedure.

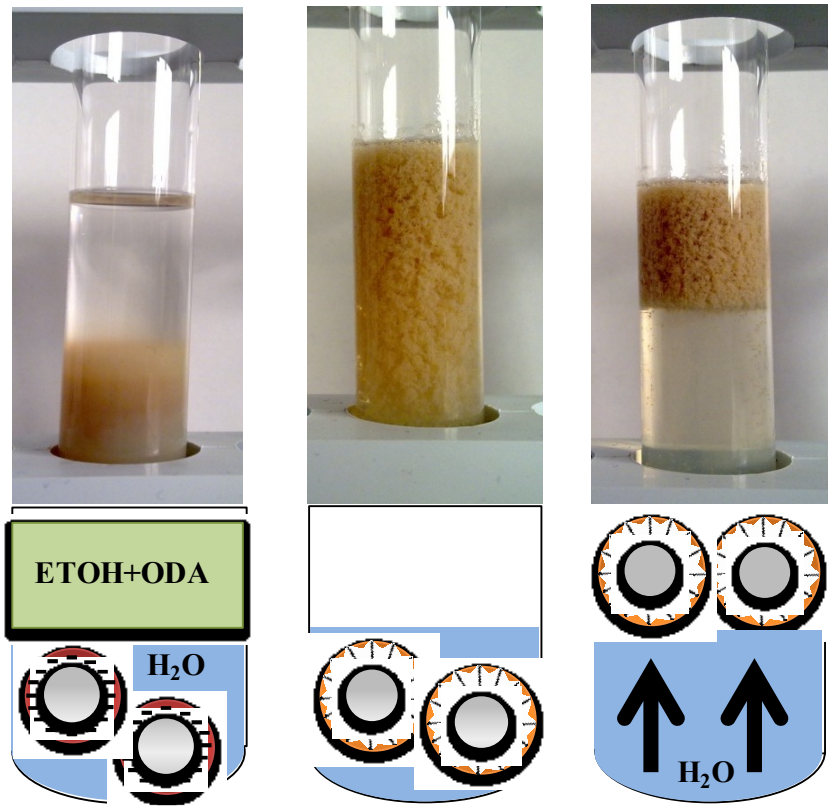

Figure 24: Nanoparticles phase transfer process: (A) the silver nanoparticles suspension (bottom phase) with the ODA ethanol solution (upper phase), (B) immediately after the vigorous shacking, (C) the solution spontaneously separated into two phase the ODA–NP (upper phase)and a mixture of water and ethanol (bottom phase).

Some preliminary experiment for the phase transfer of the LL-AgNPs were performed, showing the possibility to exchange the capping with the ODA and re-disperse the ODA-LL-AgNPs in hexane.

5.4 Conclusion

The reason for the decrease of the bilirubin SERRS intensity after the addiction of HSA was investigated. The interaction of HSA with PLL was studied using TEM, showing the formation of a HSA layer around the PLL-AgNPs. For this reason the bilirubin was no able to interact with the PLL-AgNPs.

To try to overcome this problem a phase-transfer process using an hydrophobic capping was proposed. The LM-AgNPs were coated with the ODA and re-disperse in hexane.

Some preliminary experiment shown that is also possible to transfer the LL-AgNPS in an organic phase.

The ODA-LM-AgNPs and ODA-LL-AgNPs should be characterized, the interaction with bilirubin should be studied and the enhancement properties should be tested.

5.5 References

[1] B T Doumas and T W Wu, "The measurement of bilirubin fractions in serum," *Critical reviews in clinical laboratory sciences*, vol. 28, pp. 415-445, 1991.

[2] J D Ostrow, P Mukerjee, and C Tiribelli, "Structure and binding of unconjugated bilirubin: relevance for physiological and pathophysiological function," *Journal of Lipid Research*, vol. 35, pp. 1715 - 1737, 1994.

[3] J Yang, J Y Leeb, and J Y Ying, "Phase transfer and its applications in nanotechnology," *Chem. Soc. Rev.*, vol. 40, pp. 1672 -1696, 2011.

[4] A Kumar, H Joshi, R Pasricha, A B Mandale, and M Sastry, "Phase transfer of

silver nanoparticles from aqueous to organic solutions using fatty amine molecules," *Journal of Colloid and Interface Science*, vol. 264, pp. 396 - 401, 2003.

[5] M Karg et al., "Versatile Phase Transfer of Gold Nanoparticles from Aqueous Media to Different Organic Media," *Chem. Eur. J.*, vol. 17, pp. 4648 – 4654, 2011.

[6] X Wang, S Xu, J Zhou, and W Xu, "A rapid phase transfer method for nanoparticles using alkylamine stabilizers," *Journal of Colloid and Interface Science*, vol. 348, pp. 24 - 28, 2010.

[7] Nicolae Leopold and Bernhard Lendl, "A New Method for Fast Preparation of Highly Surface-Enhanced Raman Scattering (SERS) Active Silver Colloids at Room Temperature by Reduction of Silver Nitrate with Hydroxylamine Hydrochloride," *J. Phys. Chem. B*, vol. 107, no. 24, pp. 5723-5727, 2003.

[8] P C Lee and D Meisel, "Adsorption and surface-enhanced Raman of dyes on silver and gold sols Adsorption and Surface-Enhanced Raman of Dyes on Silver and Gold Sols," *J. of Phys. Chem.*, vol. 86, pp. 3391-3395, 1982.

[9] M Potara, D Maniu, and S Astilean, "The synthesis of biocompatible and SERS-active gold nanoparticles using chitosan," *Nanotechnology*, vol. 20, p. 315602, 2009.

[10] R Development Core Team, R: A language and environment for statistical computing., 2010.

[11] L Gong, W Constantine, and Y A Chen, msProcess: Protein Mass Spectra Processing, 2009.

[12] C Beleites and Valter Sergo, hyperSpec: a package to handle hyperspectral data sets in R, in preparation for Journal of Statistical Software, R package version 0.95.

[13] J M Kirk, "Neonatal jaundice: a critical review of the role and practice of bilirubin

analysis," *Annals of clinical biochemistry*, vol. 45, pp. 452-462, 2008.

[14] W Gaoa et al., "Protein adsorption and biomimetic mineralization behaviors of PLL–DNA multilayered films assembled onto titanium," *Applied Surface Science*, vol. 257, pp. 538 - 546, 2012.

[15] H D Singh, G Wang, H Uludag, and L Unsworth, "Poly-L-lysine-coated albumin nanoparticles: Stability, mechanism for increasing in vitro enzymatic resilience, and siRNA release characteristics," *Acta Biomaterialia*, vol. 6, pp. 4277 - 4284, 2010.

[16] C D Walkeyab and C W Chan, "Understanding and controlling the interaction of nanomaterials with proteins in a physiological environment," *Chem. Soc. Rev.*, vol. 41, pp. 2780–2799, 2012.

[17] E Casalas, T Pfaller, A Duschl, G J Oostingh, and V Puntes, "Time Evolution of the Nanoparticle Protein Corona," *ACS Nano*, vol. 4, no. 7, pp. 3623 - 3632, 2010.

[18] S Goy-López et al., "Physicochemical Characteristics of Protein–NP Bioconjugates: The Role of Particle Curvature and Solution Conditions on Human Serum Albumin Conformation and Fibrillogenesis Inhibition," *Langmuir*, vol. 28, pp. 9113 - 9126, 2012.

[19] L Treuel et al., "Quantifying the influence of polymer coatings on the serum albumin corona formation around silver and gold nanoparticles," *J Nanopart Res*, vol. 14, pp. 1102 - 1114, 2012.

Chapter 6:

Coated silver nanoparticles to detect heme proteins on gold electrodes[2]

6.1 Introduction

Cytochrome-c and cytochrome b5 are heme proteins. Those small redox proteins are very similar in size and functionality as both proteins play a role in biological electron transfer processes. However, strong differences are observed in the respective binding affinities as cytochrome-c is a cationic protein and cytochrome-b5 an anionic protein [1].

Several analytical methods can be applied to understand the behavior of those heme protein. But there is not one single technique which can supply all the information required to describe adequately the cytochrome-c and cytochrome-b5 [2], since the properties of proteins are the result of complex mutual interactions between different factors often difficult to separate. For this reason, it is advantageous to

[2] Adapted from Marsich L., Sivanesan A., Kozuch J., Bonifacio A., Weidinger I. M., Sergo V., "Shell isolated nanoparticles for non invasive SER detection of protein chemistry on electrodes", In Preparation

couple different analytical techniques providing significant and complementary information, for instance electrochemistry and Raman spectroscopy.

Direct electrochemistry of cytochrome-c and in particular cyclic voltammetry (CV) has been performed since 1979 on chemically modified electrodes [3]. From CV measurements it is possible to obtain the reduction potential (E°′). This key property of all the redox proteins is related to thermodynamics and kinetics of the electron-transfer process.

The value of E°′ of cytochrome-c is very sensitive to changes occurring in the surrounding of the heme, in particular pH and ionic composition of the solvent, temperature, presence of organic solvents. Unfortunately, it does not give any structural information about these changes. In order to obtain the structural information that CV alone cannot provide the heme proteins can be studied coupling SERRS with electrochemistry.

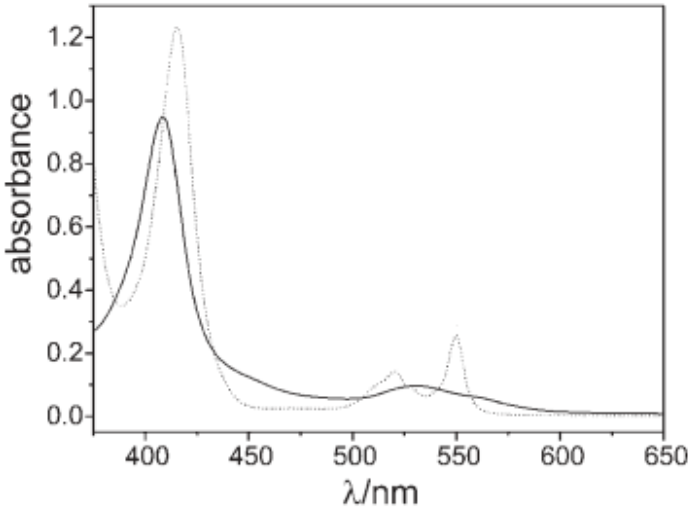

Figure 25: Absorption spectrum of cytochrome c in the reduced form (dotted line) and oxidized form (solid line) [4]

Due to their heme cofactor both proteins exhibit a strong absorption band around 400 nm [4] (Figure 25), hence a strong resonance Raman signals can be obtain with violet excitation light.

To observe the heme protein SERRS spectrum the protein should be immobilize on a nanostructured metal surface with the plasmonic frequencies in the same region of the resonance condition of the protein. To match this condition silver is to be preferred as electrode material [2].

The gold in this range of frequencies is a SERS-inactive substrate. But from the electrochemical point of view, there are several reasons to prefer gold instead of silver as electrode material [5]: (i) the mechanical polishing, which plays a crucial role in the quality and the reproducibility of the cyclic voltammetry signal, is easily performed for gold electrodes, conversely it is well known to lead to inhomogeneous silver surface; (ii) compared to gold, silver exhibits a smaller potential window; (iii) the chemical treatment to renew the gold surfaces are too aggressive to silver; (iv) gold is generally considered a better substrate for self-assembled monolayers (SAMs); (v) sulfur-containing SAMs built on gold surfaces have been widely characterized over the past decade.

The objective of this work is to develop coated silver nanoparticles (coat-AgNPs) in order to detect the cytochrome-c and cytochrome-b5 attached on a polished gold electrode using SERRS during electrochemical experiment.

During the experiments the analyte and the coated AgNPs were co-adsorbed on the working electrode in a three electrode electrochemical cell (Figure 26). The AgNPs coating is necessary to minimize the interaction between the coated AgNPs and the protein and to use the coated AgNPs exclusively for optical amplification of the protein adsorbed on a SERRS-inactive substrate.

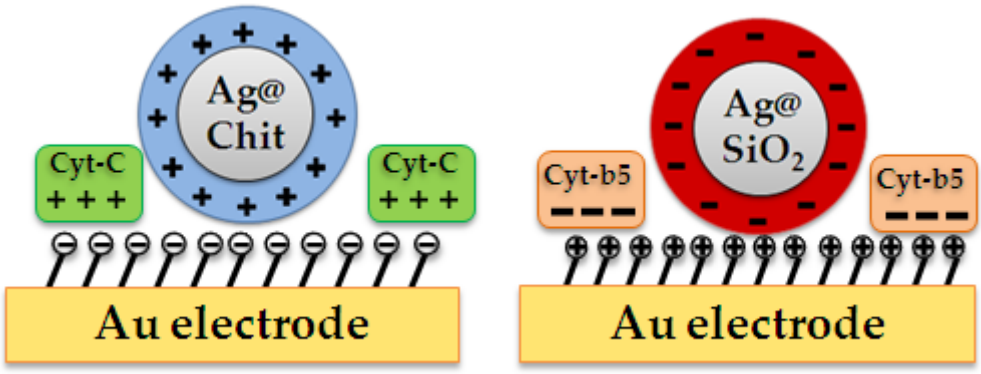

Figure 26: Schematic representation of A) chitosan coated nanoparticles (AgNPs@Chitosan) and cytochrome-c co-adsorbed on gold electrode and B) silica coated nanoparticles (AgNPs@SiO_2) and cytochrome-b5 co-adsorbed on gold electrode.

The AgNPs were prepared via seed method and subsequently coated with chitosan (AgNPs@Chitosan) or silica (AgNPs@SiO_2) in order to obtain positively and negatively charged AgNPs. The synthesis and characterization of AgNPs@Chitosan and AgNPs@SiO_2 are reported in literature [1], [6]. The coated AgNPs ability to detect selectively cytochrome-c and cytochrome-b5 only in solution has been shown [1]. It was also demonstrated that the AgNPs@Chitosan do not bind cytochrome-c, on the contrary AgNPs@SiO_2 do not interact with cytochrome-b5.

The enhancement properties of AgNPs@Chitosan and AgNPs@SiO_2 adsorbed on a electrode was evaluated using a simplified system. The spectrum intensity of a negatively charged monolayer, the mercaptobenzoic acid (4-MBA), and a positively charged monolayer, the aminothiophenol (4-ATP) was compared to the spectrum obtained electrostatically binding the coat-AgNPs to the monolayer.

Since gold is a SERRS-inactive substrate with violet excitation light, the effect of the addiction of the coat-AgNPs on the cytochrome-c spectrum and on the capability to change the protein oxidation state was evaluated using a polished silver electrode. The AgNPs coating and the SAM were chosen in order to maximize the interaction of

the protein and the coat-AgNPs with the electrode, and to minimize the interaction of the protein with the coat-AgNPs. For this reason, AgNPs@Chitosan were used in combination with mercaptoundecanoic acid (MUA) to detect the cytochrome-c, and AgNPs@SiO_2 with amino undecanethiol (AUT) to measure cytochrome- b5.
The applicability of the AgNPs@Chitosan and AgNPs@SiO_2 to detect the cytochrome-c and cytochrome- b5 on a SERRS-inactive substrate, such as gold, was evaluated.

6.2 Experimental section

6.2.1 Materials

Silver nitrate, trisodium citrate, sodium borohydride, ascorbic acid, 3-aminopropyltrimethoxysilane (APTS), sodium silicate solution, acetic acid, chitosan (medium molecular weight), 4-aminothiophenol (4-ATP) , 4-mercaptobenzoic acid (4-MBA), mercaptoundecanoic acid (MUA), absolute ethanol were obtained from Sigma-Aldrich. Phosphate buffer solution (10 mM, pH 7.00) was prepared using K_2HPO_4 and KH_2PO_4, both purchased from Sigma-Aldrich. Tris buffer solution (10mM, pH 7.5) was prepared using the TRIS purchased from Sigma-Aldrich. Horse heart cytochrome-c was purchased from Sigma-Aldrich and purified by high-performance liquid chromatography. The cytochrome b5 was separated by size exclusion chromatography after the expression of the human sulfite oxidase in E.coli TP1000 cells containing the plasmid pTG718. 11-aminoundecanethiol hydrochloride (AUT) were purchased from Dojindo, and used without further purification. All solutions were prepared with Millipore water (18MΩ, Eschborn, Germany).

6.2.2 *Nanoparticles synthesis*

Small silver nanoparticles (AgSEEDs) were synthesized by reduction of $AgNO_3$ by $NaBH_4$ following the procedure reported by Sivanesan et Al. [7]. 2 mL of 1% $AgNO_3$ and 4 mL of 38.8 mM sodium citrate were added to 200 mL of Millipore water at 0° C. After 1 min of stirring, 0.6 mL of fresh 0.01% $NaBH_4$ were slowly added dropwise under vigorous stirring. The resulting dark yellow colloidal solution was stirred for additional 3 h and stored in the dark at 4 °C. The absorption maximum will be around 390 nm.

These small nanoparticles were used as seeds for the synthesis of larger silver nanoparticles via seeding growth method adding a $AgNO_3$ and ascorbic acid[8]. Under stirring, the same volume of ascorbic acid solution (0.002% w/v) and of silver nitrate solution (0.002% w/v) were added dropwise to 3 times diluted AgSEEDs solution. The growth of the AgNPs could be controlled by amount of $AgNO_3$ and ascorbic acid added to the AgSEEDs solution.

After the addition the absorption maximum shift was checked. Two batches were prepared: one with absorption maximum at 418 nm ($AgNPs_{418}$) and one with absorption maximum 405 nm ($AgNPs_{405}$).

6.2.3 *Chitosan coated seeded nanoparticles (AgNPs@Chitosan):*

For the synthesis of AgNPs@Chitosan [1] with absorption maximum at 413 nm, 15 mL of freshly prepared 0.1% (w/v) chitosan in 1% (v/v) acetic acid solution was added to 75 mL of $AgNPs_{418}$ under hot condition (80−90 °C). The stirring was continued for 3 h, and the AgNPs@Chitosan were finally stored at 4 °C.

6.2.4 Silica coated seeded nanoparticles (AgNPs@ SiO_2):

For fabrication of AgNPs@SiO_2 [6] with absorption maximum at 413 nm a freshly prepared aqueous solution of APTS (0.4 mL, 0.2% w/v) was added to 25 mL of $AgNPs_{405}$ at pH 5.0. Under stirring, 2 mL of 2% w/v sodium silicate solution was added to the APTS capped nanoparticles. The pH was adjusted to 10.0 with sulphuric acid (0,1 M) and the solution was stirred for 24 h. Finally, AgNPs@SiO_2 were purified by centrifugation and redispersed in milliQ water and stored at 4 °C.

6.2.5 Electrode preparation

Silver or gold working electrode was always polished with 3 μm and with 0.05 μm alumina powder, sonicated and washed to remove all the polishing powder. After polishing the electrodes were immediately immerse in the monolayer solution overnight. The concentration of the monolayer solution are reported in Table 1.

Monolayer	Concentration
4-ATP	10 mM in ethanol
4-MBA	10 mM in ethanol
MUA	10 mM in ethanol
AUT	1mM in water-ethanol solution (1:4)

Table 1: concentration of the different monolayer used for coating Ag and Au electrode.

For the spectro-electrochemical experiment with cytochrome-c, the MUA coated electrodes were incubated for 30 min in the protein solution (0,5 μM cytochrome-c in phosphate buffer) and washed before the incubation for 30 min in the AgNPs@Chitosan solution (diluted 7 times). For the experiment with cytochrome-b5, the AUT coated electrodes were incubated for 30 min in the protein solution (0,5 μM

cytochrome-b5 in TRIS buffer), washed and incubated for 30 min in the AgNPs@SiO2 solution (diluted 7 times).

6.2.6 *Instumentation*

UV−vis spectra were collected with a Cary50 spectrometer between 350 and 600 nm. Samples were prepared by diluting 10× the AgSEEDs or AgNPs stock solution with Milli-Q water in a 3 mL cuvette.

The analysis system used for the spectroelectrochemical experiment was composed of an homemade electrochemical cell with three electrode: a working electrode, made of a 10 mm diameter disc of gold or silver, a platinum wire, used as counter electrode, and a reference electrode (3 M KCl Ag/AgCl). The three-electrode system was controlled with a μAutolab potentiostat (EcoChemie, Utrech, TheNetherlands).

SERRS spectra were measured with the 413 nm excitation line of a Kr^+ laser using a confocal Raman microscope (LabRam HR-800, Jobin Yvon) equipped with a N_2(l)-cooled, back illuminated charge-coupled device (CCD) detector. The laser beam was focused on the rotating electrochemical cell with a long working distance 20x objective (0.35 N.A.). SERRS spectra were acquired with a laser power of 1 mW.

6.2.7 *Spectroscopic and spectro-electrochemical measurements*

Accumulation time was 10 s for the SERS spectra of 4-ATP and 4-MBA. In this case the electrochemical cell circuit was open (no potential applied). Cytochrome-c and cytochrome-b5 SERRS spectra were collected on polished silver electrode with an acquisition time of 10 s, on polished gold electrode with a total acquisition time of 30 s. In the case of cytochrome-c to reduce or oxidize the protein, the applied potential

was – 300 mV or +70 mV respectively. The measurements of the cytochrome-b5 were performed with the electrochemical cell circuit open (no potential applied). The electrochemical cell was rotated to avoid laser induced protein degradation.

6.3 Results and discussion

6.2.8 AgNPs@Chitosan and AgNPs@SiO_2 absorbance spectra

The AgSEEDs have an absorption maximum at 390 nm (dotted black line in Figure 27A and B), as reported in literature [7].

To obtain a final absorption maximum of 413 nm (Figure 27A, solid blue line), the AgNPs absorption maximum before the chitosan coating was 418 nm (Figure 27A, dashed red line). The plasmon resonance wavelength blue shift, from 418 to 413 nm, can be attributed to the presence of the chitosan on AgNPs, and the relatively small 5 nm of this shift rules out the formation of large AgNPs aggregates.

The AgNPs absorption maximum values before the silica coating was 405 nm (Figure 27B, dashed red line). The shift of the plasmonic frequency from 405 nm to 413 nm (Figure 27B) can be attributed to the presence of the SiO_2 on the AgNPs surface, indicating that the SiO_2 coating succeeded. Also for the AgNPs@SiO_2, the relatively small red shift (5 nm) due to the SiO_2 coating exclude the AgNPs aggregation.

Figure 27 highlights that AgNPs@Chitosan and AgNPs@SiO_2 exhibit identical optical properties, in particular the absorption maximum is 413 nm, matching precisely the excitation wavelength.

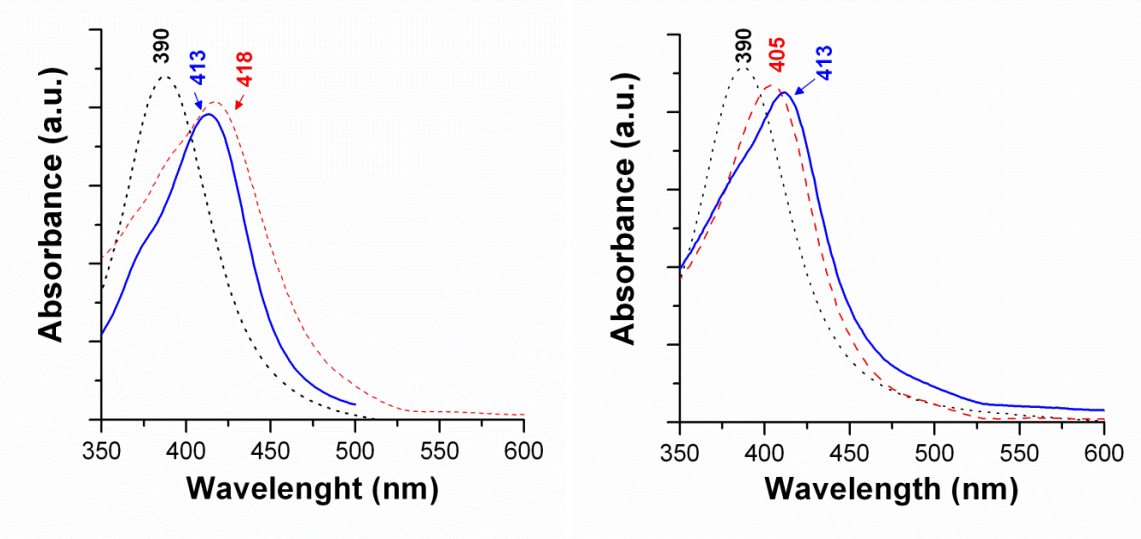

Figure 27: UV-Vis absorbance spectra of: a) AgSEEDs (dotted black line) and $AgNPs_{418}$ (dashed red line), AgNPs@Chitosan (solid blue line) ; b) AgSEEDs (dotted black line), the $AgNPs_{405}$ (dashed red line), and $AgNPs@SiO_2$ (solid blue line).

6.2.9 *Nanoparticles enhancement evaluation on polished silver electrode*

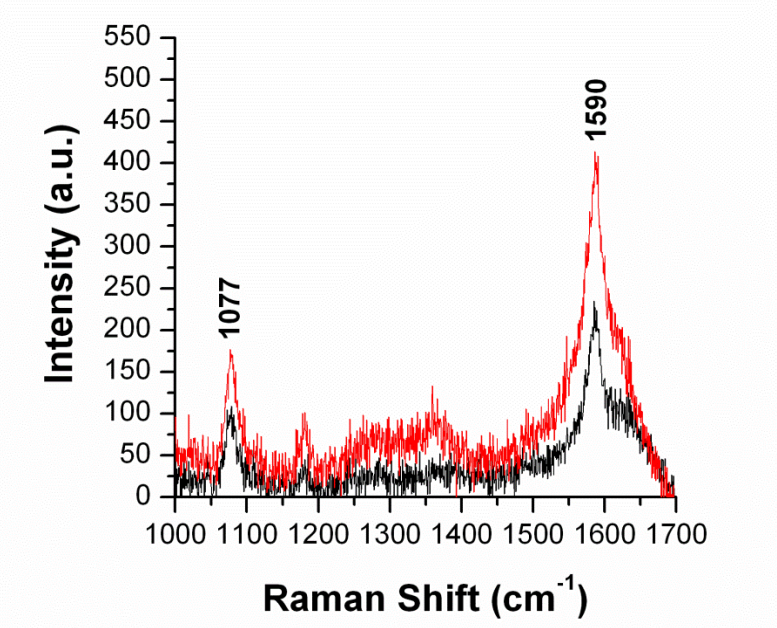

Figure 28: 4-MBA SERS spectrum on polished silver electrode (black line), 4-MBA SERS spectrum on polished silver electrode with nAg@Chitosan (red line), λexc = 413 nm, 1 mW and 5 sec.

The 4-MBA monolayer on polished silver electrode SERS spectrum (Figure 28, black line) is dominated by two strong bands at 1590 and 1077 cm^{-1}, in agreement with the data previously reported in literature [9]. Those bands are caused by the aromatic ring vibration [9]. The signal most probable is generated from some scratches that remain on polished electrode.

After the AgNPs@Chitosan addiction, the 4-MBA SERS spectrum still presented two strong band at 1590 and 1080 cm^{-1} (Figure 28, red line), and the 4-MBA SERS spectrum intensity increase 1.5 times (Figure 28).

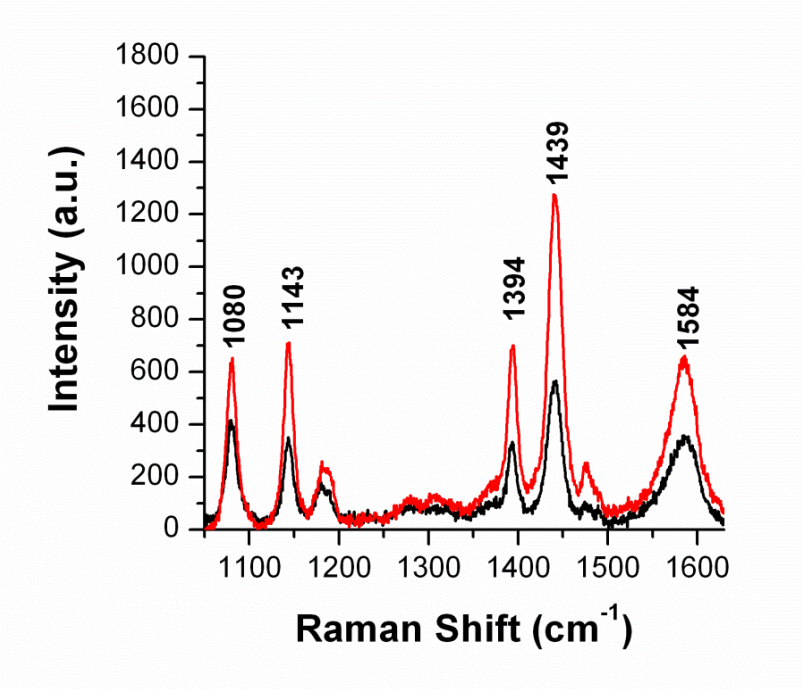

Figure 29: 4-ATP SERS on polished silver electrode (black line), 4-ATP SERS spectrum on polished silver electrode with nAg@Silica (red line), λexc = 413 nm, 1 mW and 10 sec.

The SERS spectrum of 4-ATP monolayer on polished silver electrode (Figure 29, black line) presents the same spectral features reported in literature [10,11]. Five strong bands are observed at 1584, 1439, 1394, 1143, and 1080 cm^{-1} in the SERS spectrum. According to previous study [11], the band at 1584 and 1080 cm^{-1} can be

assigned to stretching mode of C-C and C-S, the band at 1443, 1394 cm^{-1} to a combination of the stretching mode of C-C and the bending mode of C-H and the band at 1143 cm^{-1} to the bending mode of C-H. Also for the 4-ATP signal most likely is enhanced from some scratches on the polished electrode.

No changes are observable in the relative positions of 4-ATP spectral features due to the addiction of the AgNPs@SiO_2, but the overall spectrum intensity increase (Figure 29, red line). In particular the value of the ratio between the 4-ATP spectrum intensity in AgNPs@SiO_2 presence and the intensity without the AgNPs@SiO_2 was 2.

6.2.10 Effect of AgNPs@Chitosan on cytochrome c and of AgNPs@SiO_2 on cytochrome b5 spectrum

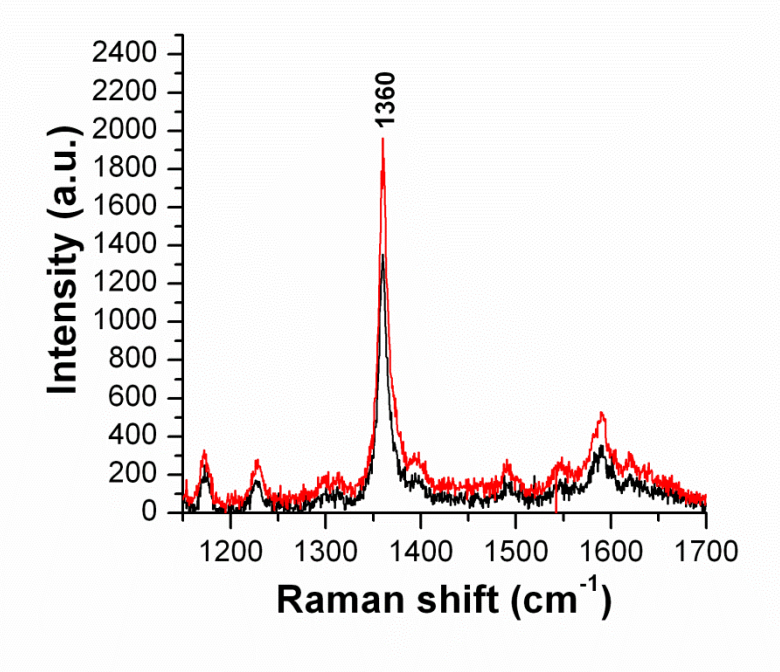

Figure 30: Cytochrome-c spectrum on polished silver electrode (dotted black line) and cytochrome c spectrum co-adsorbed with the AgNPs@Chitosan on polished silver electrode (solid red line). The SAM was MUA. The potential applied was -300 mV. λexc= 413 nm, 1 mW and 10 sec.

The cytochrome-c spectrum measured on a polished silver electrode coated with MUA at –300mV, showed a strong band at 1360 cm^{-1} (Figure 30, dotted black line), as reported in previous studies [4, 5, 12]. As for the 4-MBA and 4-ATP the signal enhancement is generated from some scrapes, derived from the polishing procedure. According to the literature [13], spectral features between 1350-1400 cm^{-1} were due to the pyrrole half-ring symmetrical stretching mode (ν_4).

If the cytochrome-c molecules were co-adsorbed with the AgNPs@Chitosan on polished silver electrode the vibrational band position did not change and the spectrum was more intense (Figure 30, solid red line), although the surface coverage of the protein was higher for the system without the NPs. In this case, the AgNPs@Chitosan enhance the cytochrome-c spectrum, without interact directly with the analyte molecules and interfering in the spectral features.

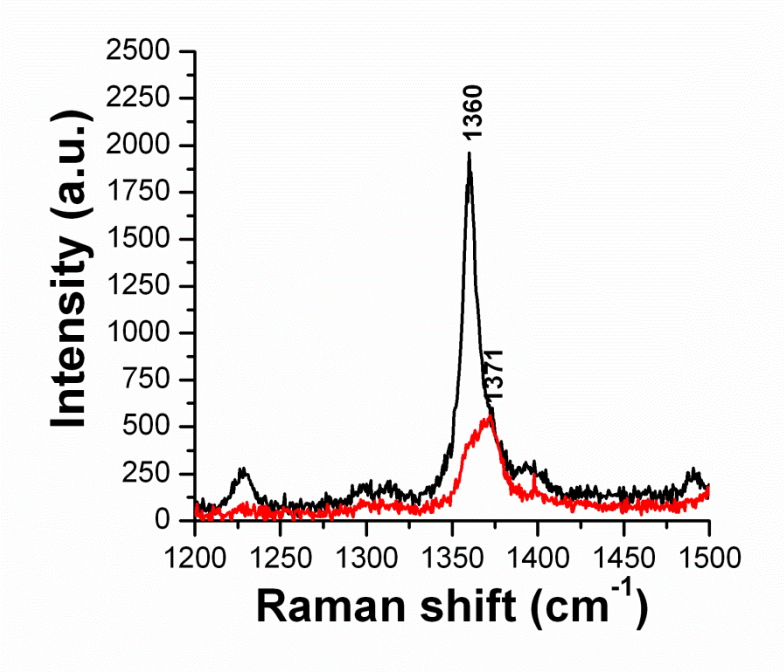

Figure 31: Cytochrome-c spectrum co-adsorbed with the AgNPs@Chitosan on polished silver electrode applying -300 mV (dotted black line) and +70 mV (solid red line). λexc= 413 nm, 1 mW and 10 sec.

SERRS spectrum at - 300 mV of the cytochrome-c co-adsorbed with the AgNPs@Chitosan still exhibits the band at 1360 cm^{-1} (Figure 31, dotted black line), typical for the reduced cytochrome-c form [2]. Consistently, the SERRS spectrum at +70 mV exhibits an increasing band at 1371 cm^{-1} (Figure 31, solid red line), typical for the oxidized cytochrome-c form [2]. Hence cytochrome-c oxidation state can be evaluated during spectro-electrochemical in the presence of the AgNPs@Chitosan.

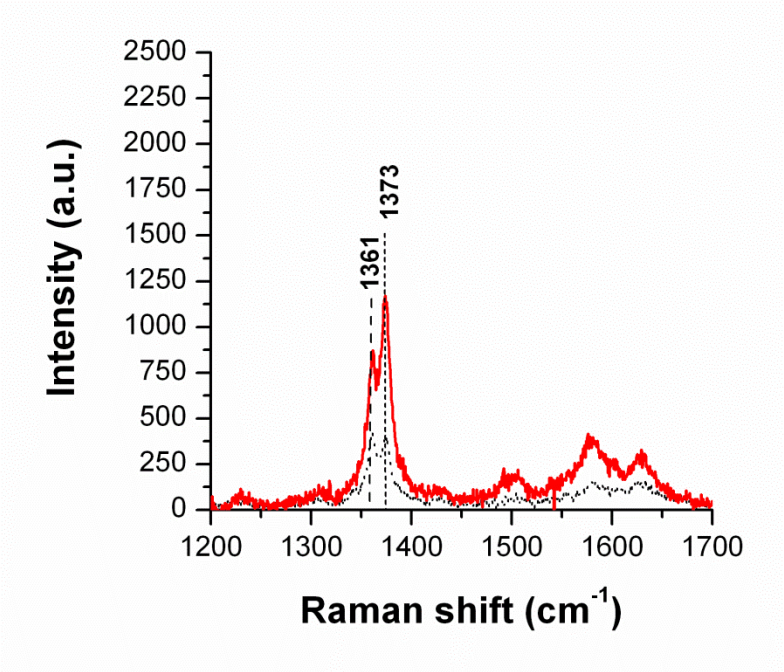

Figure 32: Cytochrome-b5 spectrum on polished silver electrode (black line) and cytochrome-b5 spectrum co-adsorbed with the AgNPs@SiO_2 on polished silver electrode (red line). The SAM was AUT. No potential applied. λexc= 413 nm, 1 mW and 10 sec.

The cytochrome-b5 spectrum measured on a polished silver electrode coated with AUT shown two strong band between 1350 and 1400 cm^{-1} (Figure 32, black line), in agreement with data reported in literature [14]. As for the cytochrome-c, those spectral features are due to the pyrrole half-ring symmetrical stretching mode (ν_4) [13] and the signal enhancement derives from few surface scratches. The band at 1361

cm^{-1} and 1373 is typical of the reduced and oxidised form, respectively [14]. The presence of the typical spectral features of both cytochrome-b5 oxidation form is in agreement with the fact that during the measurement the electrochemical cell circuit was open (no potential applied).

The SERRS spectrum of the cytochrome-b5 co-adsorbed with the AgNPs@SiO_2 on polished silver electrode (Figure 32) shows the same vibrational bands of the SERRS spectrum in the absence of the AgNPs@SiO_2. As for the cytochrome-c, the SERRS spectrum intensity increases due to the presence of AgNPs@SiO_2 (Figure 32), even if the amount of cytochrome-b5 bind to surface is higher without the AgNPs. This fact highlights the possibility to apply the AgNPs@SiO_2 for enhancing the signal of cytochrome-b5 bind to an electrode, without a direct interaction between the AgNPs and the protein.

6.2.11 Detection of cytochrome-c and cytochrome-b5 on polished gold electrode

Since gold with violet excitation light a SERRS-inactive substrate, the spectrum of cytochrome-c (Figure 33, black line) and of cytochrome-b5 (Figure 34, black line) adsorbed on polished gold electrode does not show any vibrational bands.

On the contrary, co-adsorbing the cytochrome-c with the AgNPs@Chitosan, a band at 1361 cm^{-1} is visible in the SERRS spectrum collected at -300 mV (Figure 33, red line). As said in the previous section, this band can be assigned to the cytochrome-c reduced form [2].

In the SERRS spectrum of the cytochrome-b5 co-adsorbed with the AgNPs@SiO_2 on polished gold electrode (Figure 34, red line), as for the silver electrode, are visible two bands at 1361 and 1373 cm^{-1}, assignable to the cytochrome-b5 reduced and oxidised

form respectively. Also in this case the electrochemical cell was circuit open.

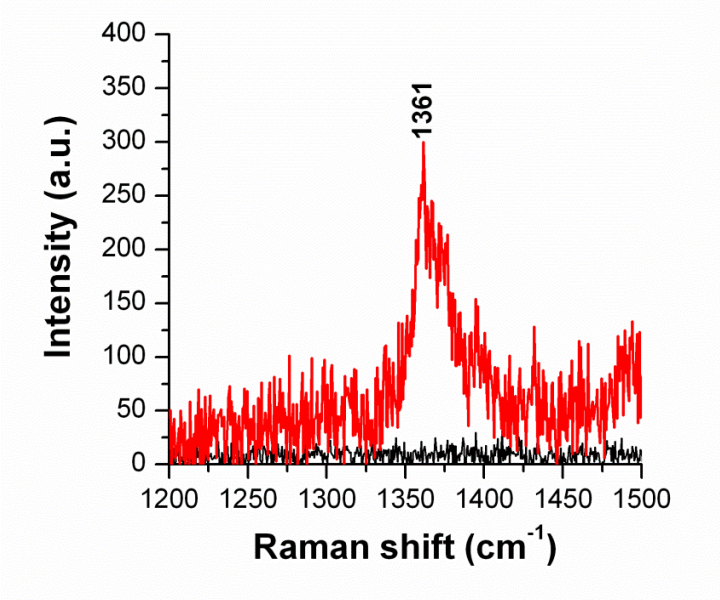

Figure 33: Cytochrome-c spectrum on polished gold electrode (black line), cytochrome-c spectrum co-adsorbed with the AgNPs@Chitosan on polished gold electrode (red line). The SAM was MUA. No potential applied. λexc= 413 nm, 1 mW and 30 sec.

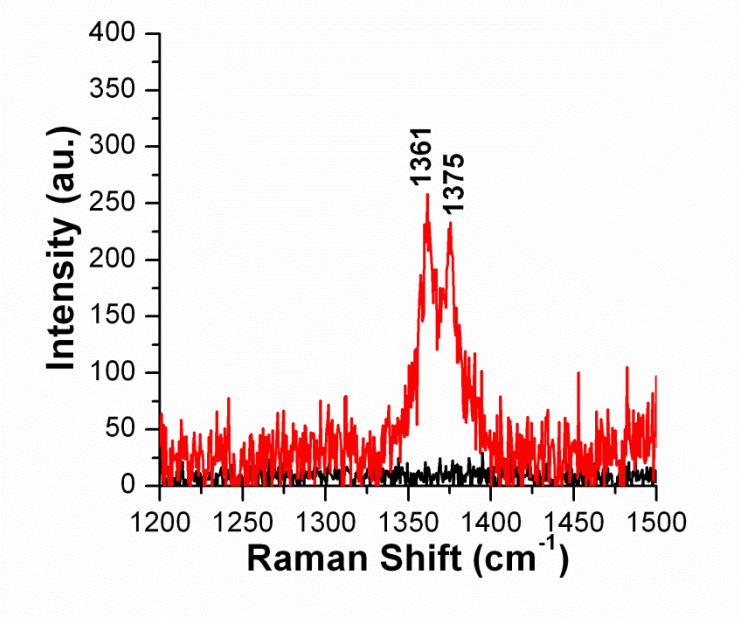

Figure 34: Cytochrome-b5 spectrum on polished gold electrode (black line), cytochrome-b5 spectrum co-adsorbed with the AgNPs@SiO_2 on polished gold electrode (red line). The SAM was AUT. No potential applied. λexc = 413 nm, 1 mW and 30 sec.

The presence of one or two bands between 1350 and 1400 cm^{-1} (Figure 33 and Figure 34, red line) demonstrate that is possible to detect the cytochrome-c and cytochrome-b5 on a SERRS-inactive substrate, such as gold, with the AgNPs@Chitosan and the AgNPs@ SiO_2 respectively.

6.4 Conclusion

In this chapter the enhancement properties of AgNPs@Chitosan and AgNPs@SiO_2 electrostatically bind to a polished silver electrode was shown. The application of AgNPs@Chitosan and AgNPs@SiO_2 to enhance the cytochrome-c and cytochrome-b5 SERRS spectrum on polished silver electrode was reported. This study demonstrate that such substrates enhance the protein spectrum without directly interact with the protein, in particular the AgNPs@Chitosan does not interfere in the cytochrome-c oxidation state evaluation. Because of the AgNPs@Chitosan and AgNPs@SiO_2 characteristics such substrates can be applied to enhance the protein signal during spectro-electrochemical experiment.

The possibility to detect cytochrome-c and cytochrome-b5 on a SERRS-inactive substrate, such as gold, thanks to the presence of AgNPs@Chitosan and AgNPs@SiO_2 was demonstrated.

6.5 References

[1] Arumugam Sivanesan et al., "Complementary Surface-Enhanced Resonance Raman Spectroscopic Biodetection of Mixed Protein Solutions by Chitosan- and Silica-coated Plasmon-Tuned Silver Nanoparticles," *Anal. Chem.*, p. 5759–5764,

2012, 84.

[2] Diego Millo et al., "Voltammetric and surface-enhanced resonance Raman spectroscopic characterization of cytochrome-c adsorbed on a 4-mercaptopyridine monolayer on silver electrodes," *Langmuir*, vol. 23, pp. 4340-4345, 2007.

[3] M J Eddowes and H A O Hill, "Electrochemistry of Horse Heart Cytochrome c ," *Journal of the American Chemical Society*, vol. 101, no. 16, pp. 4461-4464, 1979.

[4] Friedrich Siebert and Peter Hildebrandt, *Vibrational Spectroscopy in Life Science*. Weinheim: WILEY-VCH Verlag GmbH & Co.KGaA, 2008.

[5] Diego Millo, Antonio Ranieri, Wynanda Koot, Cees Gooijer, and Gert van der Zwan, "Towards combined electrochemistry and surface-enhanced resonance Raman of heme proteins: improvement of diffusion electrochemistry of cytochrome c at silver electrodes chemically modified with 4-Mercaptopyridine," *Anal.Chem.*, vol. 78, pp. 5622-5625, 2006.

[6] Arumugam Sivanesan et al., "Tailored silica coated Agnanoparticles for non-invasive surface enhanced Raman spectroscopy of biomolecular targets," *RSC Advances*, pp. 805–808, 2012, 2.

[7] Arumugam Sivanesan, Khoa H. Ly, Jacek Kozuch, Murat Sezer, and Uwe Kuhlmann, "Functionalized Ag nanoparticles with tunable optical properties for selective protein analysis," *Chem. Commun.*, pp. 3553–3555, 2011, 47.

[8] Nikhil R. Jana, Latha Gearheart, and Catherine J. Murphy, "Seeding Growth for Size Controlof 5-40 nm Diameter," *Langmuir*, pp. 6782-6786, 2001, 17.

[9] A Michota and J Bukowska, "Surface-enhanced Raman scattering (SERS) of 4-mercaptobenzoic acid on silver and gold substrates," *J. Raman Spectrosc.*, vol. 34,

pp. 21-25, 2003.

[10] J Zheng et al., "Surface-enhanced Raman scattering of 4-aminothiophenol in assemblies of nanosized particles and the macroscopic surface of silver," *Langmuir*, vol. 19, pp. 632-636, 2003.

[11] M Osawa, N Matsuda, K Yoshii, and I Uchida, "Charge Transfer Resonance Raman Process in Surface-Enhanced Raman Scattering from p-Aminothiophenol Adsorbed on Silver: Herzberg-Teller Contribution," *J. Phys. Chem.*, vol. 98, pp. 12702-12707, 1994.

[12] D. H. Murguda and Peter Hildebrandt, "Electron-transfer processes of cytochrome c at interfaces. New insights by surface-enhanced resonance Raman spectroscopy," *Acc. Chem. Res.* , vol. 37, pp. 854-861, 2004.

[13] S. Hu, K. M. Smith, and T. G. Spiro, "Assignment of protoheme resonance Raman spectrum by heme labeling in myoglobin," *J. Am. Chem. Soc*, vol. 118, pp. 12638-12646, 1996.

[14] M. Sezer et al., "Redox properties and catalytic activity of surface-bound human sulfite oxidase studied by a combined surface enhanced resonance Raman spectroscopic and electrochemical approach," *Phys. Chem. Chem. Phys.*, vol. 12, pp. 7894–7903, 2010.

[15] Agata Krolikowska and Jolanta Bukowska, "Surface-enhanced resonance Raman spectroscopic characterization of cytochrome-c immobilized on 2-mercaptoethanesulfonate monolayers on silver," *J. Raman Spectrosc.*, vol. 41, pp. 1621-1631, 2010.

[16] Yi-Fan Huang et al., "Shell-isolated nanoparticle-enhanced Raman spectroscopy of pyridine on smooth silver electrodes," *Electrochimica Acta*, vol. 56, pp. 10652-

10657, 2011.

[17] D-X Lin et al., "Shell-isolated nanoparticle-enhanced Raman spectroscopy: nanoparticle synthesis, characterization and applications in electrochemistry," *Journal of Electroanalytical Chemistry*, p. In press, 2012.

Chapter 7:

Conclusions

In this doctoral thesis the preparation of SERS active substrates, consisting in coated silver nanoparticles, and the implementation with biological samples have been reported.

In literature silver nanoparticles of different sizes and shapes have been synthesized using various methods, such as chemical reduction, chemical replacement, electrochemical reduction, photochemical, thermal decomposition, and ultrasonic decomposition methods. At the beginning of this work the simplest and the most widely used chemical reduction method proposed by Lee-Meisel was chosen. Citrate reduced silver nanoparticles were coated with poly-L-lysine and consistent results from UV-vis, TEM, z-potential, DLS and SERS microscopy prove that poly-L-lysine forms a positively-charged polymer layer around the nanoparticles, without inducing their aggregation. This study demonstrates that the poly-L-lysine coated AgNPs can be used as stable, reproducible and efficient SERS substrates for detection and quantification of the anionic chromophore bilirubin in aqueous solutions in a range from 10 nM to 200 nM.

Unfortunately, the poly-L-lysine coated AgNPs cannot be applied for indirect quantification of bilirubin cell up-take. Indeed the bilirubin spectrum intensity decreases if the bilirubin solution is prepared using a buffer suitable for cell growth (pH 7.4).

Since the reason of this decrease could be the different protonation state of poly-L-lysine at a lower pH, the poly-L-lysine was substituted with two positively charged polymers, that contain a quaternary nitrogen atom (poly-N^+). Thanks to the presence of the quaternary nitrogen atom, the charge of this polymer does not depend on pH. The citrate reduced AgNPs were coated with P(AAm-DADMAC) and P(DADMAC) and the possibility to detect 100 nM bilirubin concentration with this substrates was demonstrated. To obtain more reproducible and stable SERRS substrates, the citrate reduced AgNPs have been immobilized on a glass slide using the P(AAm-DADMAC) and P(DADMAC). Those promising positively charged substrate should be characterized and optimized for measuring bilirubin.

The poly-L-lysine coated AgNPs have been applied to measure bilirubin in the serum. With this purpose, the interaction of human serum albumin with the poly-L-lysine was studied using TEM, showing the formation of an albumin layer around the poly-L-lysine coated AgNPs. Hence the bilirubin is not able to interact with the poly-L-lysine coated AgNPs.

Whereas the bilirubin is considered hydrophobic and to avoid the albumin layer around AgNPs, the citrate reduced AgNPs were coated with an hydrophobic capping, the octadecylamine, and re-disperse in hexane. In this part of the work a faster and more reproducible synthesis method was also considered. Some preliminary experiments have showed that is possible to transfer also the AgNPs synthesized using Leopold-Lendl procedure into an organic phase. The citrate

reduced AgNPs and Leopold-Lendl AgNPs coated with octadecylamine should be characterized, the interaction with bilirubin and albumin should be investigated and the enhancement properties should be evaluated.

To obtain shell isolated nanoparticles that can be used exclusively for optical amplification without directly interact with the analyte, AgNPs were prepared via seed growth method and subsequently coated with chitosan or silica. This study demonstrates that chitosan and silica coated AgNPs enhance the SERRS spectrum of heme proteins on polished silver electrode during spectro-electrochemical experiments. In particular the chitosan coated AgNPs does not interfere in the cytochrome-c oxidation state evaluation. The possibility to detect heme proteins on a SERRS-inactive substrate, such as gold, thanks to the presence of chitosan and silica coated AgNPs was demonstrated. Because of their characteristics, such substrates could be applied to spectroscopically detect surface bound molecules on random surfaces, coupling SERS spectroscopy with other analytical techniques, providing significant and complementary information.

Acknowledgements

I would like to sincerely thank my advisor, professor Valter Sergo, he has been a mentor to me during these years of doctoral research. I am also very grateful to Alois Bonifacio for his scientific advice and knowledge and many insightful discussions and suggestions. Thanks to Claudia, that has shared with me her experience and knowledge about R and analytical chemistry.

An important period of my PhD has been the Berlin one. I would like to thank Peter Hildebrandt and Inez Weidinger. They welcomed me in their lab and they gave me the great opportunity of working at the TUB. I would like also to thank all the members of the Hildebrandt group especially Arumugam and Diego, that shared with me their protocols and knowledge about heme proteins.

I would like to thank Sabina Passamonti (Life Science Dept. University of Trieste) and Lovro Ziberna as well as Claudio Tiribelli, Cristina Bellarosa, Pablo Giraudi and Silvia Gazzin (Centre for Liver Studies, Trieste) for sharing their knowledge about bilirubin.

I would like to sincerely thank my friends for supporting me during the years and my parents and Alessio for their support and encouragement throughout my study.